Design and Characterization of Resist and Mold Materials for Electron-Beam and Nanoimprint Lithography

by

Celal Con

A thesis
presented to the University of Waterloo
in fulfillment of the
thesis requirement for the degree of
Master of Applied Science
in
Mechanical Engineering

Waterloo, Ontario, Canada, 2011

© Celal Con 2011

AUTHOR'S DECLARATION

I hereby declare that I am the sole author of this thesis. This is a true copy of the thesis, including any required final revisions, as accepted by my examiners.

I understand that my thesis may be made electronically available to the public.

Abstract

Electron beam lithography (EBL) and Nanoimprint Lithography (NIL) are the promising tools for today's technology in terms of resolution capability, fidelity and cost of operation. Achieving highest possible resolution is a key concept for EBL where there is a huge request in applications of nanotechnology for sub-20 nm feature sizes. Defining features at these length scales is a challenge, and there is a large demand for resist that is not only capable of giving high resolution but also having low cost and ease of process. In this work I studied Polystyrene (PS) which is an alternative organic e-beam resist in terms of ease of process and resolution capability. I examined the process of electron-beam exposure and attempted to characterize the factors that affect the achieved resolution and sensitivity. Besides this work, I designed and fabricated a new type of mold for NIL since mold fabrication is a key factor for NIL technology. The resolution of NIL process depends on the mold features and polymer mold technology received great attention in terms of cost of fabrication and process, fidelity, and reliability. I used MD 700 Fluoropolymer as a new type of polymer mold which was believed to be a good candidate for the polymer mold of high throughput NIL.

Acknowledgements

It is a great pleasure to thank those who made this thesis possible.

This thesis would not have been possible without the contributions of the following people, all of whom I feel extremely lucky to have had the opportunity to work with:

I would like to thank Professor Dr. Mustafa Yavuz for supervising my thesis, and for his continuous support of my study and research, motivation, valuable comments, assistance, and insights into this project.

I owe my deepest gratitude to Professor Dr. Bo Cui for his trust, encouragement, helpful advice and valuable discussions. I greatly appreciated his tremendous help in improving my English writing skills on top of the scientific ones. His enthusiasm, immense knowledge and guidance helped me in research and writing of this thesis.

I am grateful to Professor Dr. Baris Fidan and Dr. Norman Zhou for being a member of my thesis committee, and for his advice, assistance, and insightful comments and feedbacks on this thesis.

I would also like to thank Siqi Ma for her great help in handling the experiments while I went back to my home country to get married.

Special thanks to Jian Zhang. He was a great friend, and always willing to help me no matter time or day of the week. His assistance was priceless when I was in trouble with atomic force microscopy and scanning electron microscopy.

Richard Barber and Nina, we are so privileged to have someone like you keeping the Giga-2 Nano Lab and Watlab's scanning electron microscopy facility running and helping all the students, thanks for all your attentions.

I am deeply grateful to Professor Dr. Said Eren San, from Gebze Institute of Technology-Turkey, supervising me on Nanotechnology and sharing his valuable ideas, detailed and constructive comments and important support throughout this work.

My sincere thanks to Professor Dr. Mehmet Parlak, from Middle East Technical University, giving me a reference letter, and his ideals, knowledge and logical way of thinking have had a remarkable influence on my academic career.

A very special thanks to Professor Dr. Ahmet Kilic, from Nigde University-Turkey, for his priceless support throughout this work; his guidance and contributions have been of great value in this study.

Financial support of this study by the Republic of Turkey, Ministry of Education, which provided me a scholarship, is gratefully acknowledged.

Finally, I am greatly indebted to my wife, Emel. Words fail me to express my appreciation to her, but her dedication, encouragement, faith and love have taken the load off my shoulder. She was my source of motivation for always giving me strength and hope throughout this work. My world is so much better with you.

Dedication

To my family

Table of Contents

List of Figures

List of Tables

Chapter 1
Electron Beam Lithography

1.1 Introduction

Nanotechnology has started to attract attention in late 1960s as a new branch of technology. Richard Feynman has led people to think about entering a new field of physics when he gave his famous talk at California Institute of Technology (CalTech) on "There is plenty of room at the bottom" in 1959 [Feynman, 1960]. After this talk, there has been much effort in the field of nano technology. Although making things smaller was seen imaginary in these days, Tom Newman achieved writing the first page of Charles Dickens's novel, "*A tale of two cities",* with a reduction factor of 25000 using Electron Beam Lithography in 1985 [Newman, 1986]. Decreasing the dimensions of the patterned functional materials has opened a new era in fabrication of high-performance and cost-effective materials as integrated circuits (IC), storage devices, displays, bio sensors and advanced materials [Saavedra, 2010]. Photolithography, which is the process of the minimum feature size scales with the wavelength of exposure light, has been used for many years in patterning most of the functional materials as ICs, MEMS, sensors, LEDS, and so on. Although there has been improvement in photolithography for the last 3 decades that has pushed the production line into the 32 nm era [Wang, 2010], there is still a need for further improvement. At reduced wavelength, photolithography is hampered by the materials including masks, resists and lenses [Wang, 2010]. According to Moore's Law, the numbers of transistors that are practically placed on an IC will double every two years [Moore, 1965]. Thus, new non-optical lithographic techniques such as electron beam lithography (EBL), ion beam lithography (IBL), and X-ray lithography etc. have superseded the optical technique [Pain, 2006; Yamomato, 2000; Lee, 1998]. EBL is a direct writing technique without using mask which is capable of obtaining a higher resolution than any other tools or optical microscopes

[Grigorescu, 2009, Saavedra, 2010]. In this work, we will give an overview on the working principle of EBL and its capabilities. After that, high resolution patterns by EBL using polystyrene (PS) negative tone resist will be discussed.

1.2 Electron Beam Lithography

Electron beam lithography (EBL), which is popular with its excellent resolution capability, low cost, high reliability and ability to write reproducible structures over large areas, is now capable of achieving sub-10 nm resolution patterns [Grigorescu, 2009]. Electron Beam Lithography (EBL), which is a maskless lithography technique based on the electron beam source, has its roots in Scanning Electron Microscopy (SEM) and becomes the most useful tool for nanofabrication due to its small wavelength and small probe size.

Electron beam can be focused to spot size less than 5 nm using electron optics which is extremely powerful more than photolithography. Associated with de Broglie wavelength, wavelength of the electron can be estimated by using equation 1 below:

$$\lambda = \frac{1.226}{\sqrt{V}}(nm)$$

Wavelength of the photon beam is calculated by equation 2:

$$\lambda = \frac{hc}{eV} = \frac{1.24}{V}(\mu m)$$

For comparison, it can be said that an electron beam has 1.2 nm wavelength for 1 eV whereas a photon beam has thousand times larger (1.22 μm) wavelength than the electron beam.

Electron beam resists that are basically polymeric materials are sensitive to the electron beam. One can create desired patterns by switching on and off the beam followed by the selective etch of resist by using solvent due to chemically modified structure of the resist. EBL has developed in late 1960s along with the Scanning Electron Microscope [Cui, 2005], and has been improved throughout the years with improvements of SEM. Figure 1.1 is a schematic view of an electron beam lithography system representing its complexity. Today, EBL is the most popular nano-patterning technique for academic research and prototyping.

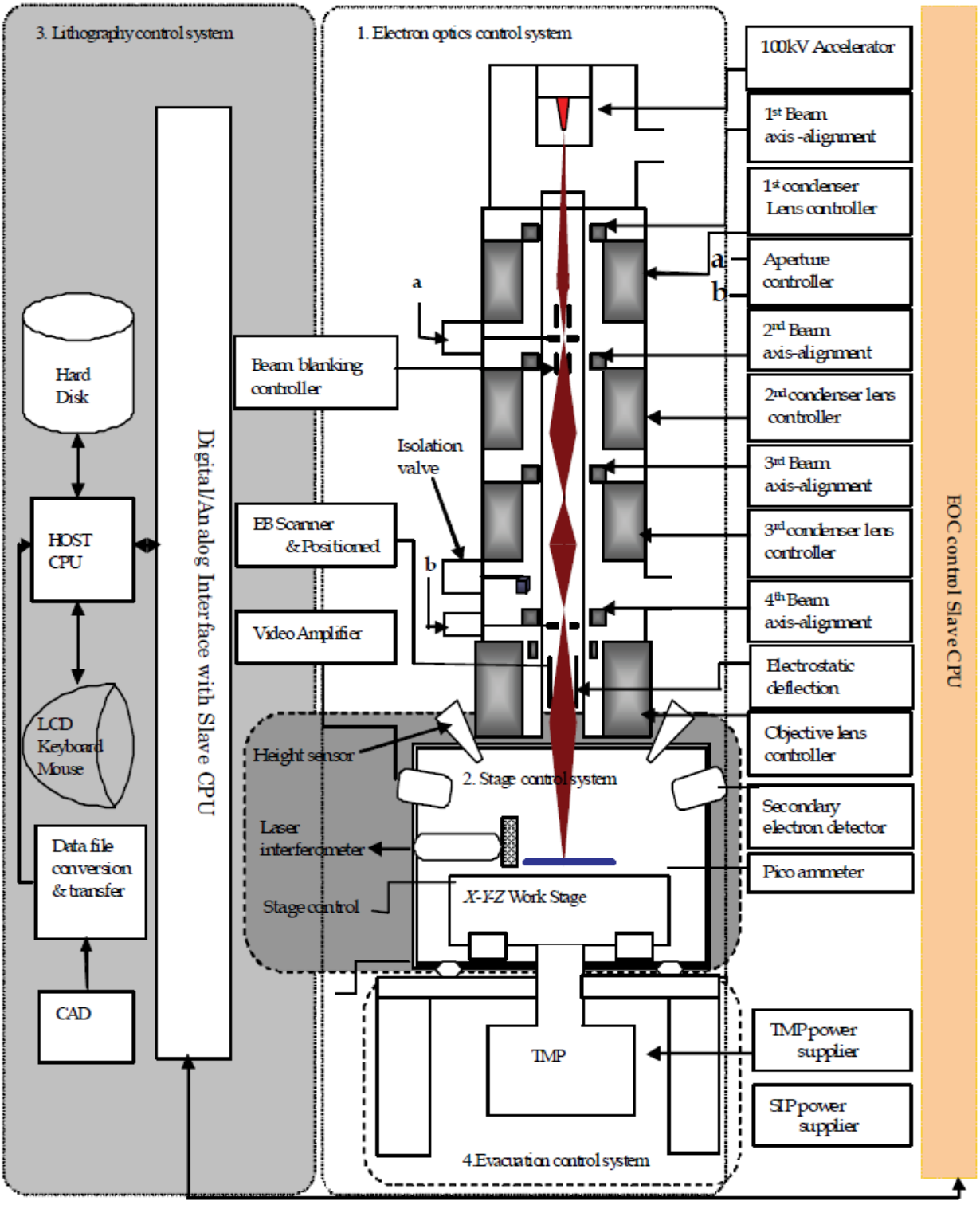

Figure 1.1 Major components of high-energy electron beam lithography system [Wang, 2010]

1.3 Fundamentals of Electron Beam Lithography (EBL)

This section gives an introduction to fundamental factors of EBL including electron beam source, electron accelerator, aberrations and limits on electron beam spot size, EBL systems, and proximity effect and how to reduce it, resists and developers and their properties, and important parameters for high resolution EBL resists.

1.3.1 Electron Beam Lithography Systems

The usage of electron beam lithography (EBL) started in late 1960s when SEM system was developed [Cui, 2005]. The application of EBL system has basically relied on the invention of the electron sensitive resists, that is, some materials would be affected by exposure to the electrons where the principle is similar to the photolithography. There have been many improvements in EBL systems and materials used together with the semiconductor technology, and different types of EBL systems now have been developed and used for industry and research. Working principles of SEM-based/converted EBL systems and e-beam direct writer systems are alike. In figure 1.2, Raith 150^{Two} Direct Write EBL system is shown.

Figure 1.2 Raith 150^{TWO} Direct Write Electron Beam Lithography Systems [Raith, 2011]

SEM based/converted systems have a beam blanker and hardware controller. Some has an additional laser system for height controller and focus correction with perfect integration to the system. The acceleration voltage can be increased up to 30 kV. In addition to the SEM based systems, Direct Write EBL systems can have 100 kV acceleration voltages with high reproducibility, automatic and continuous writing for few days, but it costs much more than SEM based systems.

1.3.2 Working scheme of the EBL

EBL process has three steps (figure 1.3); resist coating, exposure and development. Resists can be divided into two categories with respect to the reactions of the electron beam: positive and negative. Positive resists are removed by the developers after electron beam exposure, whereas negative ones remain. Resists and developers will be discussed in detail in the following sections.

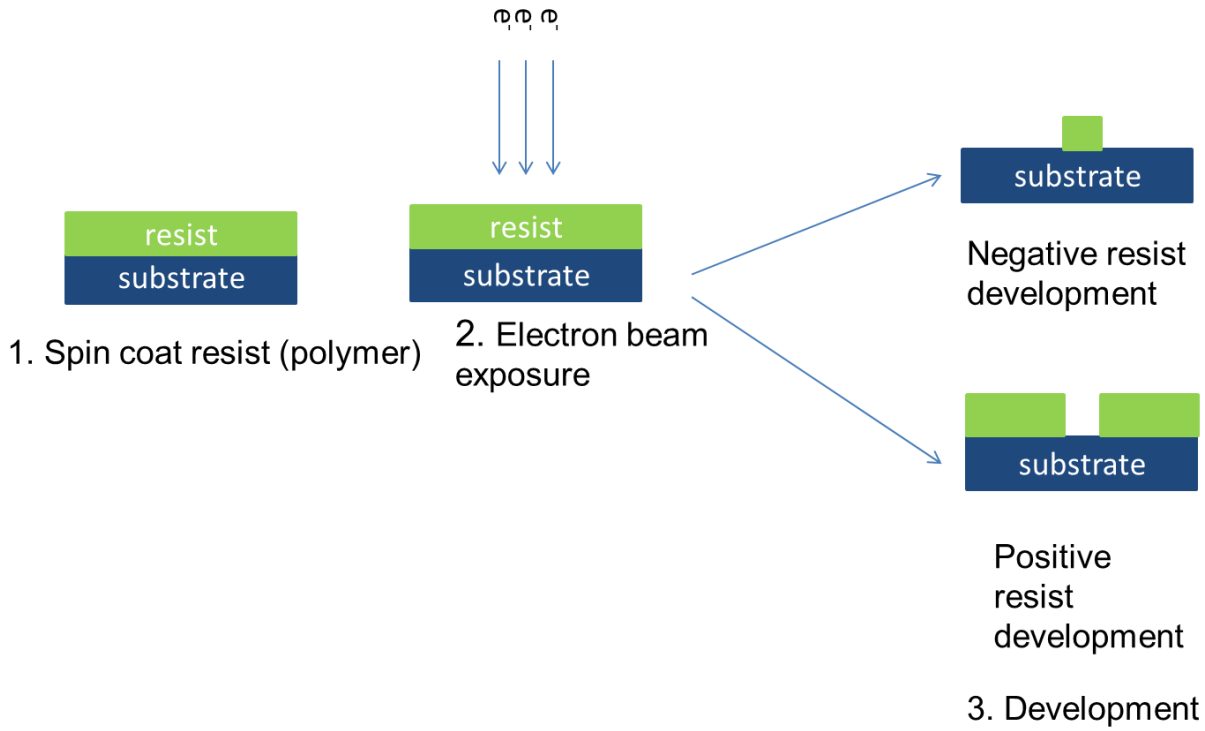

Figure 1.3 Working scheme of EBL: resist coating, e-beam exposure and development by solvent

For different applications, various substrates such as Si, SiO2, Si3N4, quartz crystal, etc. with distinct shapes up to 8" can be used in several EBL tools aforementioned.

1.3.3 Scan systems and beam shapes

In EBL writing systems, there are two different writing strategies that can create pattern on the resist: raster scan and vector scan (figure 1.4). For raster scan, the beam moves in one direction and desired pattern is written by switching on and off the beam by beam blanker. Raster scan is very simple, fast and repeatable operation, but during the exposure, it is very hard to adjust the focus. It is good for making photo mask where focus will not be a hard issue. For vector scan, beam is switched on only

over the desired area to be written, and the beam can move along x and y directions in order to write the next area. It leads to faster writing compared to raster scan for sparse patterns since unwritten parts are skipped. For vector scan, dose can vary easily from shape to shape which makes it useful for nanolithography and Research and Development [Madou, 1997].

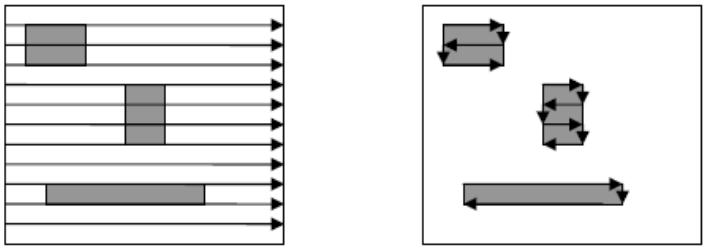

Figure 1.4 Scan systems for EBL

In EBL system, beam shape can vary in two different ways: Gaussian (figure 1.5a) and shaped (figure 1.5b) beams. Gaussian beam is a rounded beam, and focused to spot size as small as possible for high resolution, which is important for R&D, though it is slow due to small pixel size of the patterned area (about 10 nm). Shaped beam uses the combination of the apertures to make an electron beam rectangular yet variable shape to write faster for large pixel areas. The most IC pattern pixels are large (100 nm), therefore using shaped beam is much faster than using Gaussian beam [Cui, 2005]. Shaped beam only works for vector scan mode in EBL.

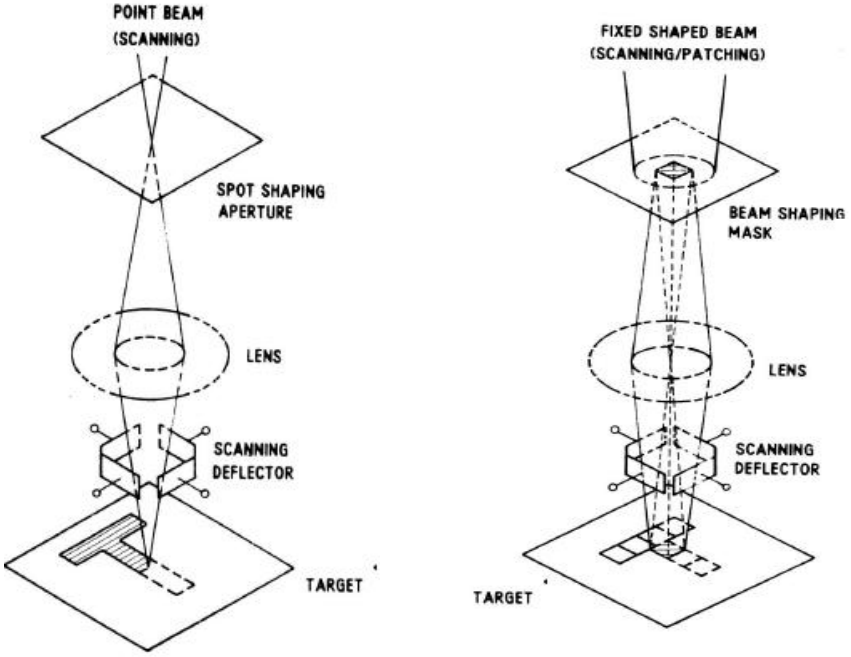

a) b)

Figure 1.5 a) Gaussian type beam and b) Shaped beam system

1.3.3.1 Principles of Electron Optics

Electron-optical control system is the main part of the EBL system. It generates a highly focused electron beam with high current density allowing the patterning of resists. It consists of 9 different components as shown in the figure 1.6: electron gun, electron gun alignment, condenser lens, beam blanker, zoom lenses, stigmator, beam aperture, projection lenses, and deflectors.

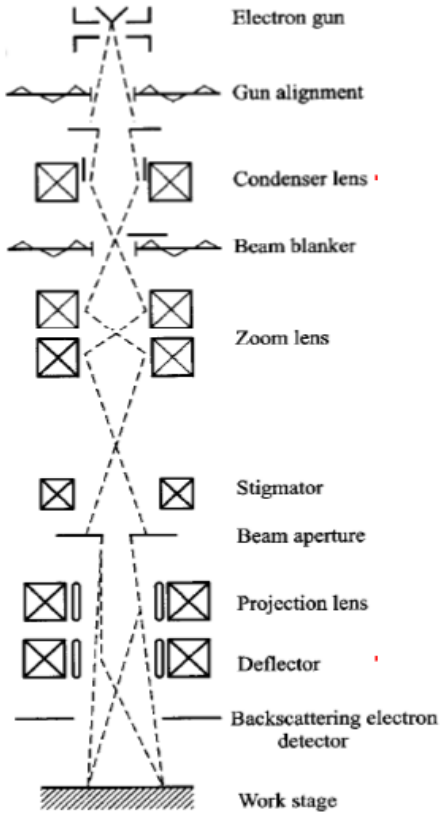

Figure 1.6 Scheme of complete electron optical system in e-beam lithography column

1.3.4 Electron Beam Source

An electron gun (source) is a portion of the electron optics of the SEM that extracts and accelerates electrons pulled out from the filament to a certain amount of energy. It consists of two components: a cathode for emitting electrons by gaining additional energy from heat or electrical field, and a lens to focus the emitted electrons into a beam, called as cathode lens [Wang, 2010, Gemma, 2008]. Figure 1.7 is a schematic view of the electron beam source, and here C is the cathode, E is the extraction electrode and A1 and A2 are the lenses.

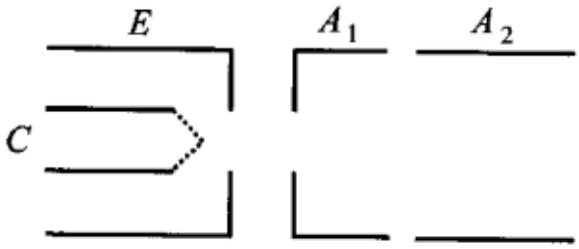

Figure 1.7 Electron Beam source scheme

For the electron beam source, virtual source size, brightness and energy spread of emitted electrons are the three key parameters. For SEM applications, smaller virtual source size is desired due to the demagnification needs. In figure 1.8a and 1.8b, two different types of electron sources are shown, and it can be said that the field emission cathode is a better source due to its higher brightness.

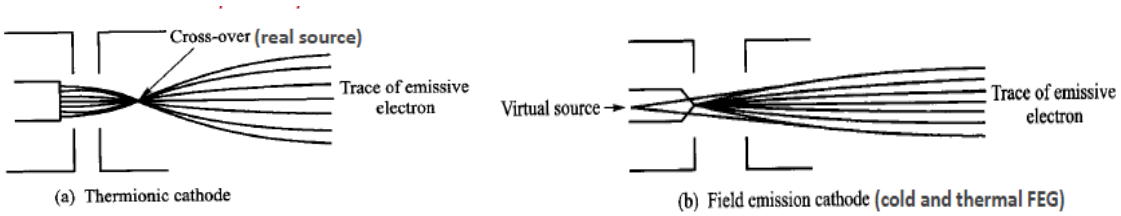

Figure 1.8 a) Thermionic cathode and b) Field emission cathode

Principally, brightness, which is the current emitted per unit area per solid angle, is equivalent to intensity in optics, and it is an important parameter for high-emission intensity and high resolution [Gemma, 2008]. For tungsten (W) thermionic emission source brightness is around 10^5 A/cm^2/rad. The energy spread of a W thermionic emitter is about 2.5 eV, and 1eV for LaB_6, thus LaB_6 is a better emitter source, though it is also more costly then W source. Sharpness of the source size is an

important parameter to get the best focus of the beam for high resolution. Basically, there are three types of electron gun sources: thermionic emission, field emission and Schottky guns. In Table 1.1 and Table 1.2, some of the filaments used in electron gun sources and their properties are listed.

In thermionic electron guns, electrons are extracted by the heating of conducting materials. Thermionic gun sources are listed in Table 1.1, as Tungsten (W) (figure 1.9) and LaB_6. At 2700 K (for Tungsten material), electrons gain enough thermal kinetic energy at the cathode surface, to overcome the energy barrier (equal work function) and to free escape from the cathode into space, in order to become free electrons. Once they escape from the tip, they are extracted by electric field generated by nearby extraction electrodes. Current density of the beam strongly depends on the temperature of the tip and work function of the material.

Figure 1.9 Tungsten (W) filament

Table 1-1 Characteristics of different types of filaments [Gemma, 2008]

Source type / Working principle	Filament material	Brightness ($A/cm^2/rad$)	Source size	Energy dispersion (eV)	Vacuum level (Torr)	Filament temperature (K)
Tungsten thermoionic	W	$\sim 10^5$	25 μm	2-3	10^{-6}	~3000
LaB_6 thermoionic	LaB_6	$\sim 10^6$	10 μm	2-3	10^{-8}	~2000-3000
Thermic field emission (Schottky)	Zr/O/W	$\sim 10^8$	20 nm	0.9	10^{-9}	~1800
Cold field emission	W	$\sim 10^9$	5 nm	0.22	10^{-10}	Ambience

Table 1-2 Characteristics of some filaments [Zhou, 2007]

Emitter type	Thermionic	Thermionic	Cold FE	Schottky FE
Cathode materials	W	LaB_6	W	ZrO/W
Operating temperature (K)	2800	1900	300	1800
Cathode radius (μm)	60	10	<0.1	<1
Virtual source radius (nm)	15,000	5000	2.5	15
Emission current density (A cm^{-2})	3	30	17,000	5300
Total emission current (μA)	200	80	5	200
Brightness	10^4	10^5	2×10^7	10^7
Maximum probe current (nA)	1000	1000	0.2	10
Energy spread at cathode (eV)	0.59	0.40	0.26	0.31
Energy spread at gun exit (eV)	1.5–2.5	1.3–2.5	0.3–0.7	0.35–0.7
Beam noise (%)	1	1	5–10	1
Emission current drift (% hr^{-1})	0.1	0.2	5	<0.5
Vacuum requirement (Torr)	$\leq10^{-5}$	$\leq10^{-6}$	$\leq10^{-10}$	$\leq10^{-8}$
Cathode life (h)	200	1000	2000	2000
Cathode regeneration	Not required	Not required	Every 6–8 h	Not required
Sensitivity to external influence	Minimal	Minimal	High	Low

In field emission (cold) type guns, electrons are tunnelled out from Tungsten tip due to high electric field (10^8 V/cm) obtained by using a very sharp tip (100 nm) and high voltage (figure 1.10). Field emission type gun operates at room temperature, thus it is called as cold type gun. As electrons are pulled out by electric field through a tunnelling process, current density of the emitted electrons is independent from the tip temperature.

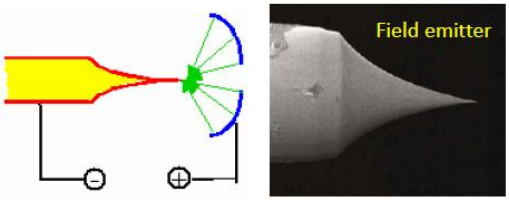

Figure 1.10 Field Emission Gun

For cold field emission gun, small beam spot size can be achieved since the high enough electric field exists only the tip apex. It needs an ultra-high vacuum, which is also important to keep the tip clean for an efficient field emitter source and to prevent arc-over at tip apex. At 10^{-6} Torr, a monolayer of gas which leads organic contamination and instability of the beam is deposited in just 5 seconds on the tip, and at 10^{-10} Torr within 5-10 minutes. In order to overcome this problem, a flashing process can be performed, where the tip is heated for a few seconds to desorb the gas. However, the process does not last long, typically 4-8 hours, which is considered ineffective for EBL; thus, cold field emission gun is not appropriate for EBL, whereas it is best for SEM imaging where current instability is act as a major issue. Advantages of this type of gun are having short switch time (less than ns), and being durable for 5 years which is good for SEM applications.

Another type of the gun is called Thermic Field Emission (Schottky) type electron source. Tungsten is a typical source for this kind of gun. A Schottky is actually a field assisted thermionic source, and it is not truly an emission gun (figure 1.11) since the tip used is blunt and there is no emission without heating.

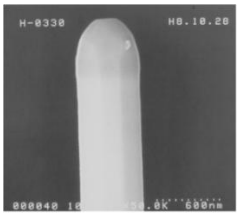

Figure 1.11 Schottky type electron source

In Schottky emitter, electric field reduces the work function (energy barrier) of the source. Work function can be reduced further by adding ZrO_3. In Schottky gun, cathode acts as a thermionic emitter, thus it has to be kept in operating condition at 1750 K, and its life time is 1-2 years. Schottky emitter has a high current density and stability, thus it is the best choice for electron beam lithography. One important issue in Schottky emitter is that there is no problem with contamination, which is undesirable in EBL, since it is always hot to burn of any organic contaminations.

1.3.4.1 Electron Accelerator

Once the electrons are emitted from the emission gun, beam enters into the acceleration system where acceleration can be reached up to 100 kV. Acceleration voltage is of great importance for high aspect ratio EBL patterning since the high aspect ratio pattern can be accomplished by the higher acceleration voltage as plainly seen in figure 1.12 [Wang, 2010].

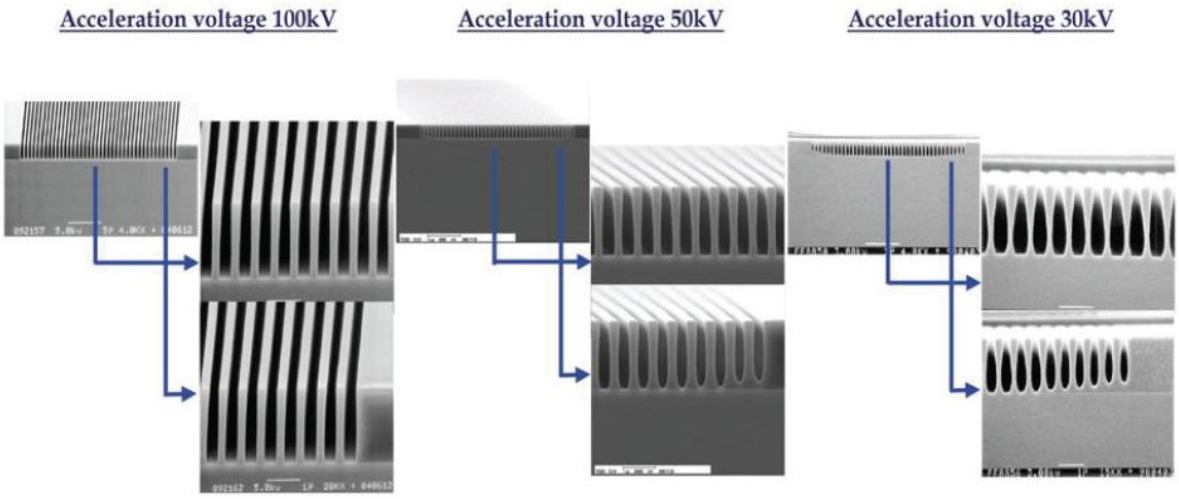

Figure 1.12 Patterns created by EBL with different acceleration voltages [Wang, 2010]

1.3.4.2 Electromagnetic Lenses

There are 4 magnetic lenses (figure 1.13) in the system. The 2nd and 3rd electromagnetic lenses that function as zoom lenses are placed after the focusing lens in order to keep focus point constant on the 4th lens called objective lens.

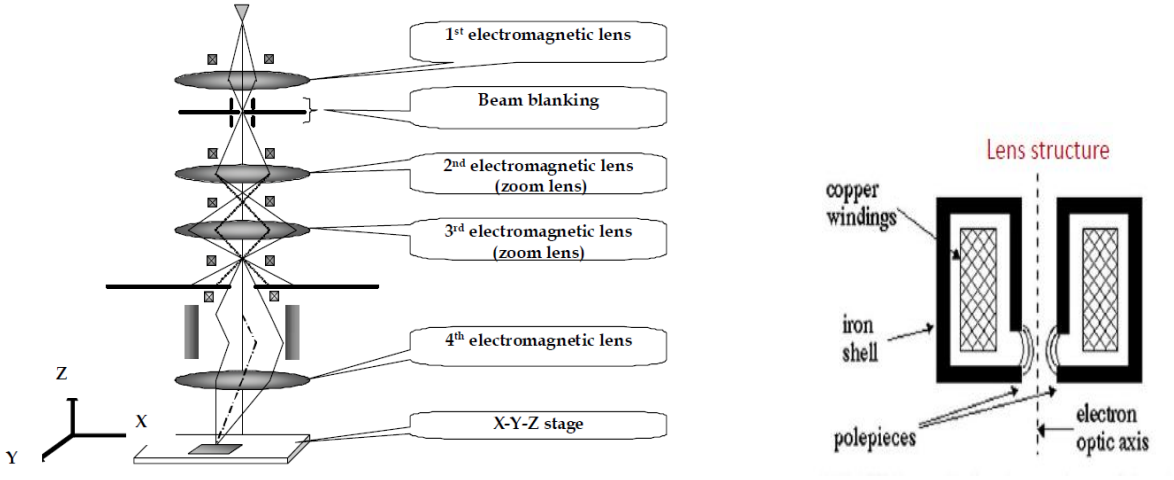

Figure 1.13 Cross-sectional drawing of electromagnetic lens system and lens structure

Once the current is applied on the wire around the cylindrical iron core, magnetic field is then created around the coil, and this makes the system to act as a magnetic lens.

1.3.4.3 Aberrations and Limits on Electron Beam Spot Size

All lenses are not ideal, and they have some deviation from its ideal state called as aberration. Astigmatism is one of the aberrations arisen during the beam adjustment. It happens when electron beam is not equally focused in X and Y directions. In figure 1.14, the difference between elliptical shaped beam and astigmatism corrected beam is shown, and their differences in SEM images can readily be seen. The reason behind astigmatism is the error in the mechanical machining of the lens components which leads to the elliptical beam shape, and it can be amended by an astigmatism corrector located after the electromagnetic lenses [Wang, 2010, Cui, 2005].

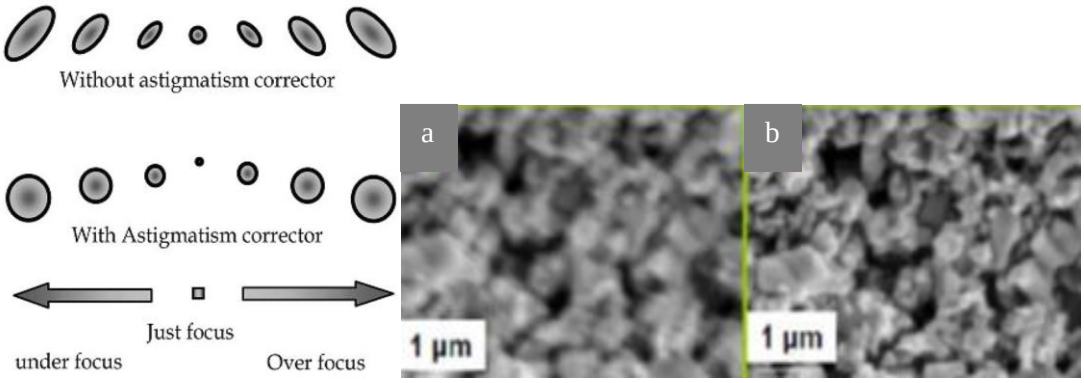

Figure 1.14 Comparisons of beam-forms on the sample and resulted SEM images. a) Before stigmation correction and b) after stigmation correction [Wang, 2010]

Ideal electron spot size is given by:

$$d_0 = \left(\frac{4i}{\pi^2 \beta} \right)^{\frac{1}{2}} \alpha^{-1}$$

Where i is the beam current, β is the brightness of the electron beam, and α is the half angle subtended by the lens aperture.

One aberration is the spherical aberration of the beam which is directly proportional to the spread angle of the beam. The spot size contribution of spherical aberration (ds) is given by:

$$d_s = 0.5\ C_s.\alpha^3$$

where C_s is the spherical aberration constant for a well-designed magnetic lens, and α is the numerical aperture of the lens.

Chromatic aberration is caused by the energy dispersion of the electrons ($\Delta E/E$) of due to the energy spread of gun emission and Coulomb interactions of electrons. The spot size contribution of chromatic aberration (d_c) is given by:

$$d_c = C_c.\alpha.\ (\Delta E/E) \qquad (C_s \text{ is a constant})$$

Diffraction is another sort of aberration. As known, electrons are waves, and diffraction limited crossover that they create at focal point by a minimum diameter is given by:

$$d_f = \lambda / \alpha$$

Diffraction is a significant factor when the beam energy is low. From de-Broglie wavelength, as energy of the beam decreases, wavelength of the beam increases (0.04 nm at 1 kV and 0.0078 nm for 25 kV).

Once all the contributions in quadrature are summed up, total beam diameter can be determined using the equation below:

$$d_{tot}^2 = d_o^2 + d_s^2 + d_c^2 + d_f^2$$

It can be concluded that EBL system can be optimized by using a reasonable beam current, the highest stable voltage, and the smallest working distance in order to have high-resolution patterns.

1.3.5 Proximity Effect and How to Reduce It

When the electron beam enters the resist/substrate media, beam has an interaction with electrons and heavy particles such as substrate nucleus, and this interaction results in the elastic and inelastic collision of the beam with resist (figure 1.15) [Wiederrecht, 2010]. Many of the electrons face with elastic scattering known as small angle forward scattering which increases the electron beam size in the resist. Few electrons experience with backscattering which is referred to as inelastic scattering.

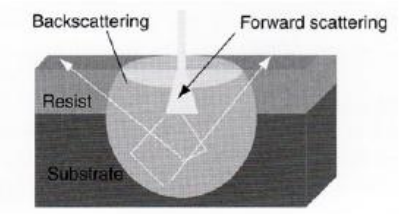

Figure 1.15 Illustration of interaction of electrons (forward and backward scattered) with resist-coated wafer

Most of the electrons penetrate into the substrate instead of being absorbed by the resist, leading to inelastic scattering. Depending on the atomic number of the substrate atoms, a 10 % to 40% of the high energy electrons are backscattered, and this results in an additional exposure of the resist besides the primary beam exposure (shown as in figure 1.16). This is called as electron beam lithography proximity effect [Gemma, 2008].

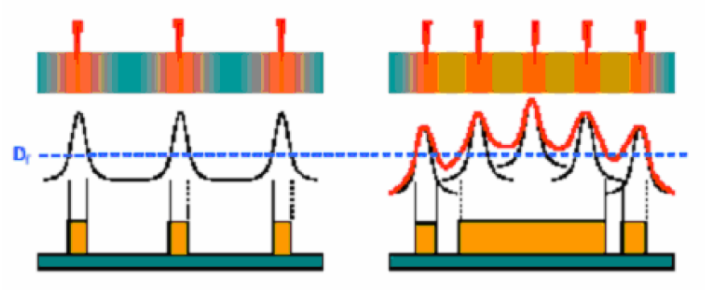

Figure 1.16 Illustrations of patterns created by normal and additional exposure [Gemma, 2008]

The sum of the backscattering and forward scattering electron beam distributions gives Gaussian distribution which was defined by Chang to calculate the result of the proximity effect on the exposure. The equation is given by [Chang, 1975, Cord, 2009]:

$$f(r) = \frac{1}{\pi(1+\eta)}\left[\frac{1}{\sigma_f^2}\exp\left(-\frac{r^2}{\sigma_f^2}\right) + \frac{\eta}{\sigma_b^2}\exp\left(-\frac{r^2}{\sigma_b^2}\right)\right]$$

Where η is the ratio of the backscattering to the forward scattering

σ_f is the forward scattering range parameter, and

σ_b is the backscattering range parameter which determines the proximity effect.

In order to reduce the proximity effect, one can make dose correction or adjust the pattern design. It can also be minimized by using high energy beam. As seen in figure 1.17, forward and back scattering are minimized or "diluted" at 100 kV compared to 30 kV beam energy [Wang, 2010].

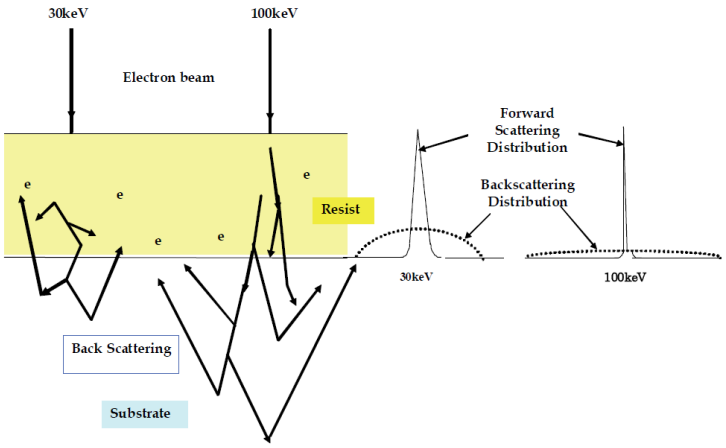

Figure 1.17 Illustration of scattered electron behaviour at 30 kV and 100 kV accelerated beam [Wang, 2010]

Another way to minimize the proximity effect is to use specific systems as multilayer resist, inorganic resists or to do the lithography on membrane that is "transparent" to electrons.

1.3.6 High Resolution E-beam Resists

Many types of resists have been developed during the past decades for electron beam lithography, and categorized into two groups in terms of chemical behaviour: organic and inorganic resists. Organic resists which consist of carbonhydrates are typically polymeric materials, and Poly methyl methacrylate (PMMA), ZEP, polystyrene (PS), and poly l-butane sulfone (PBS) are common types of organic resists. Unlike organic resists, inorganic resists are monomeric materials, and under e-beam exposure, their chemical structure is changed leading to different dissolution rate during the development procedure. Some examples of inorganic resists are Hydrogen silsesquixane (HSQ), Lithium fluorine (LiF), and Aluminium floride (AlF_3), etc [Saavedra, 2010]. Some of the resists are illustrated in figure 1.18.

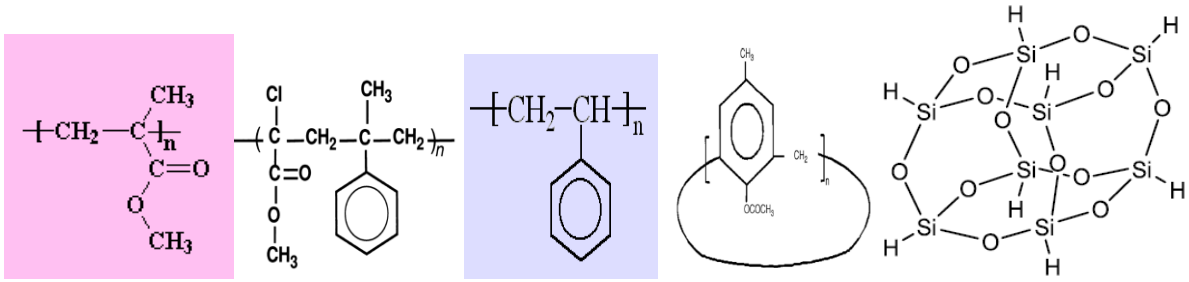

Figure 1.18 Chemical structure of PMMA, PBS, PS, Calixarene, and HSQ

Resists have basically two roles in lithography: they are used either to transfer the pattern by lift off or to protect the covered substrate from etching or ion implantation [Zhou, 2007].

Electron Beam Lithography resists are classified as positive and negative resists, as seen in Table 1.3. Resists where exposed portions are removed by a suitable solution (developer) after e-beam exposure are called positive resists, and they usually have high molecular weights. PMMA is the first developed resist for e-beam lithography, and is still most commonly used e-beam resist. PMMA has high molecular weight which ranges from 50,000 to 2.2 million g/mol (Nano PMMA and Copolymer, PMMA Resist Data Sheet, MicroChem Corp.), and is mixed with chlorobenzene solvent [Zhou, 2007]. It can be used as a positive and negative e-beam resist depending on the e-beam dose used. PMMA has high resolution capability, and Cord achieved 10 nm line width using PMMA as an e-beam resist (figure 1.19) [Chang, 1975, Cord, 2009].

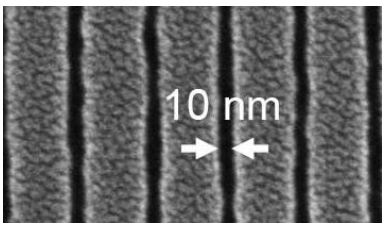

Figure 1.19 10 nm lines achieved by using PMMA positive resist [Cord, 2009]

Once exposed to e-beam, the polymeric chain are broken and form polymeric structure with lower molecular weight. Reduced M_w PMMA is soluble in the developer, whereas unexposed part of PMMA is insoluble. MIBK-IPA solution is the standard developer for PMMA. Last but not least, PMMA has a high contrast (4-8), low sensitivity (50-500 μC/cm2), and unlimited shelf life.

Table 1-3 Some popular e-beam resists and their properties [Wiederrecht, 2010]

Common EBL resists with their properties and uses

Resist	*Supplier*	*Tone*	*Sensitivity ($\mu C/cm^2$) at 100 kV*	*Developer(s)*	*Characteristics*
PMMA (high molecular weight)	Microchem	Positive	900	Cellosolve Methanol 3:7 or MIBK:IPA1:3 or IPA:Water (conc. varies)	High resolution, single layer or top of Hi/Lo bilayer, liftoff
PMMA (low molecular weight)	Microchem	Positive	800	Cellosolve Methanol 3:7 or MIBK:IPA1:3 or IPA:Water (conc. varies)	High resolution, bottom of Hi/Lo bilayer, liftoff
Copolymer (MMA/MAA)	Microchem	Positive	300	Same as above	Large undercut profile for liftoff when used as bottom layer with PMMA on top
Zep520	Zeon Chemicals	Positive	300	Hexyl Acetate, n-Amyl Acetate, or Xylenes	High resolution, good etch resistance
Zep7000	Zeon Chemicals	Positive	80	3-Pentanone Diethyl Malonate	Fast, good for making masks
NEB31	Sumika Materials	Negative	80	0.26N TMAH	Fast, chemically amplified resist
HSQ	Dow Corning	Negative	1000	0.26N TMAH	High resolution, good etch resistance, flowable oxide
Calixarene	Synthesized	Negative	10 000 or higher	Xylenes, IPA, MIBK	High resolution, good etch resistance

ZEP is one of the organic positive tone resists for EBL, which is developed by ZEON in Japan [Cui, 2005]. It is composed of methyl styrene and chloromethyl acrylate copolymer. It possesses similar properties to PMMA. Anisole is a typical solvent for ZEP type e-beam resists. Nishida has achieved 50 nm lines with 1.5 μm pitch using ZEP-520 (figure 1.20). ZEP is five times more sensitive (20-50 $\mu C/cm^2$) than PMMA, and it has very high contrast, as well [Nishida, 1992]. However, it is more expensive than PMMA with its shorter shelf-life (one year).

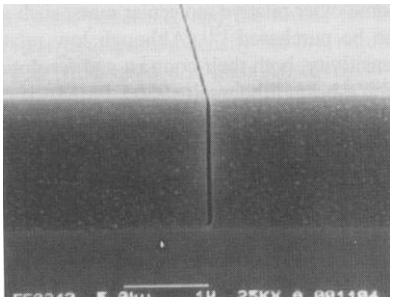

Figure 1.20 50 nm wide line with 1.5 micrometer depth achieved with ZEP resist [Nishida, 1992]

Resists which are called negative e-beam resists are insoluble in developers after e-beam exposure. Negative e-beam resists form reverse patterning compared to positive e-beam resists. Calix[n] arene is a negative tone resist for e-beam lithography. Calix[n]arene has a cylic structure, and its molecular size is less than 1 nm [Saavedra, 2010]. Xylene is a typical developer for calixarene. Although the required dose for calixarene is 20 times higher than PMMA, calixarene is preferred for some applications such as pillar array fabrication. For instance, Fujita achieved 15 nm diameter and 35 nm period dot array for data storage applications by using calixarene resist (figure 1.21) [Fujita, 1996].

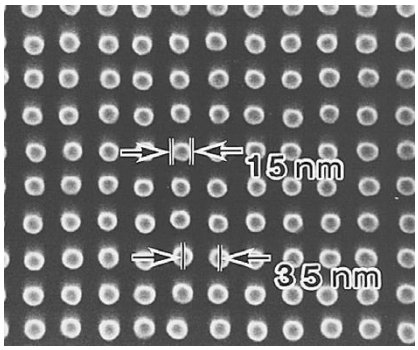

Figure 1.21 15 nm diameter and 35 nm period dot array with using calixarene resist [Fujita,1996]

SU-8 is one of the organic negative tone resists. It is chemically amplified resist which can also be used for photolithography applications and 3D structures due to its chemical properties. Although it has a low contrast and resolution, it is 100 times more sensitive than PMMA, which makes it extremely popular. Using SU-8 negative resist, Bilenberg achieved 24 nm line width using a 100 kV EBL system (figure 1.22) [Bilenberg, 2001].

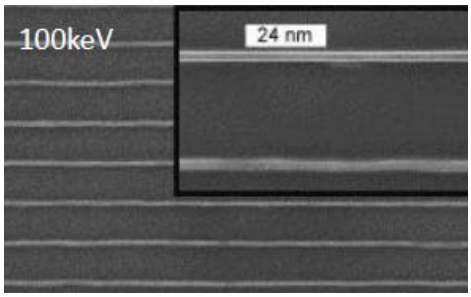

Figure 1.22 24 nm wide line achieved by using SU-8 negative resist [Bilenberg, 2001]

HSQ is an inorganic negative tone resist for e-beam lithography. It is provided by Dow Corning Corporation [Cui, 2005]. HSQ has a short shelf life and high cost in comparison to all other resists. HSQ is known as a resist that gives a high resolution, high contrast, and sensitivity as PMMA. For instance, Yang et al achieved 4.5 nm half pitch lines with 10 nm thick HSQ resist (figure 1.23) [Yang, 2009].

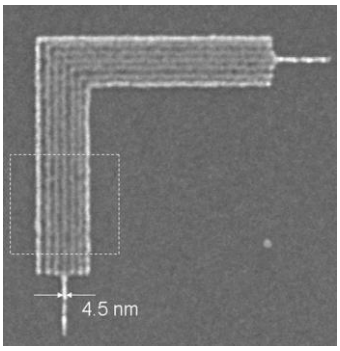

Figure 1.23 4.5 nm half pitch lines with 10 nm thick HSQ negative resist [Yang, 2009]

On the other hand, HSQ is a very unusual resist because it is not developed by a solvent but a chemical reaction. After exposure, un-exposed HSQ reacts to diluted NH_4OH or NaOH developer to produce H_2 and the development stops once it reaches the saturation point. In addition, all the processes for EBL such as spin coating, baking, e-beam exposure and development has to be performed promptly due to its instability.

1.4 High Resolution Electron Beam Lithography

Resolution that means the capability of resolving very small features is the goal of nanofabrication. Electron Beam Lithography is capable of sub-10 nm resolution. Considering the properties of resists, there are several parameters that e-beam resists must possess in order to become a good candidate for high resolution nanolithography.

Electron exposure dose is the number of electrons per unit area exposed on the resist to define a pattern. Electron dose is usually expressed in $\mu C/cm^2$, and each lithographic process has its own optimum conditions.

Sensitivity is the response of the resist to the e-beam dose, and it varies depending on the substrate used, development temperature, and the strength of the developer. As seen in the Table 1.4, developer type and concentration affect the sensitivity and resolution of PMMA. The number of backscattered electrons increases due to high atomic number of the substrate, resulting in an increased the sensitivity of the resist. For high resolution e-beam resist, its sensitivity is usually low. So there exists trade-off between resolution and resist sensitivity.

Table 1-4 Influence of developer concentration on the sensitivity & resolution of the resist

Developer concentration MIBK:IPA)	Sensitivity	Resolution
1:3	Low	Extremely high
1:2	Medium	Very high
1:1	High	High
Pure MIBK	Very high	Low

Resist's contrast determines resist's capability for high resolution and high-aspect ratio structures. It can be readily calculated from the remaining thickness of the resist after development with respect to exposed dose. Contrast, γ, is given by the equation:

$$\gamma \equiv \frac{1}{\log_{10}(D_1 / D_0)}$$

Where D_1 is the dose at which resist is 100% removed by developer (for positive resist), and D_0 is the dose at which 0 % of resist is removed. The contrast curve for positive resists will be resembled in figure 1.24a, in figure 1.24b for negative resist. Sensitivity can also be defined from the same curve, typically equal to D_1. Most resists have contrast range between 2-10, and PMMA has contrast range from 6 to 9 which makes it a good resist for a high resolution EBL [Wiederrecht, 2010].

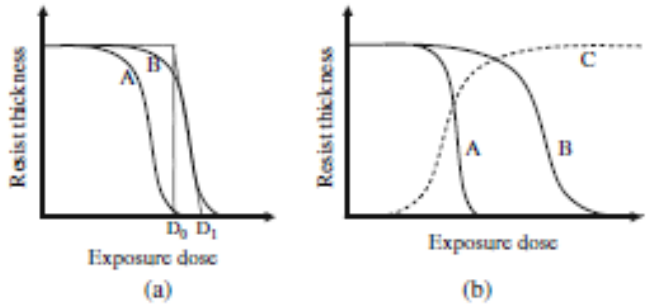

Figure 1.24 Contrast curves for a) positive and b) negative resists, respectively

Chapter 2
High Resolution Electron Beam Lithography using Polystyrene Negative Tone Resist

2.1 Motivation

Modern lithographic techniques such as EBL, NIL and FIB lithography are being widely used as top-down fabrication tools for research and development, nanostructured device fabrication such as ICs, biosensors, MEMS/NEMS, LEDs, biosensors, etc. [Grigorescu, 2009; Schift, 2008; Tseng, 2004] Among them, EBL is the most popular one since there is no need for mask as NIL which affects the cost of fabrication and capability, and it is faster than FIB. Also, e-beam can remain well focused below 10 nm beam size even with nA beam current which is desired for fast writing. EBL is capable of direct writing with high resolution and dense pattern. For EBL, positive resists are typically used resists and PMMA is the most popular one since it is easy to process and it has low cost, unlimited shelf life, and good stability. However, negative resists can be preferable for some applications such as fabrication of hole arrays in a metal film. Unfortunately, there is no negative resist as popular as PMMA. As discussed in Chapter 1, there are popular negative resists such as HSQ, SU-8, and calixarene. SU-8 is chemically amplified resist which has good sensitivity but low contrast which affects the resolution besides its high cost. Calixarene is also chemically amplified resist and it generates acids. Although it has high resolution it is not preferable due to its low sensitivity. HSQ, which Yang et al achieved 9 nm pitch lines, is inorganic resist [Yang, 2009]. It is unstable and spin coating, baking, exposure, and development must be done quickly. In addition, since it has short shelf life, it has high cost. Thus, there is no negative resist that can be as popular as PMMA. Polystyrene, where chemical structure is in figure 2.1, is a negative resist that forms three dimensional networks by crosslinking upon exposure of e-beam, and this makes it a suitable resist for investigation on high

resolution EBL [Ma 2011, Ku, 1969]. Polystyrene has longer shelf life and much more stable than conventional resists such as HSQ. Austin et al has already achieved 40 nm period lines using low molecular weight polystyrene resist, however, there is a much need for investigation of the resolution and sensitivity. In this chapter, high resolution and high sensitivity PS negative resist have been studied.

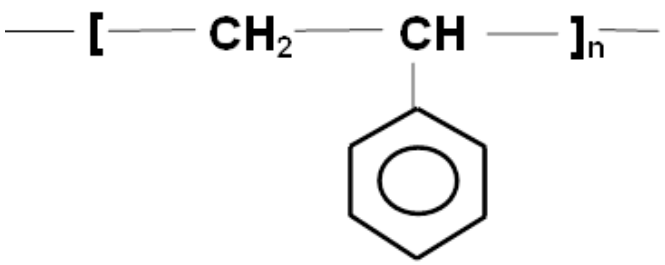

Figure 2.1 Chemical formula for Polystyrene

2.2 High resolution electron beam lithography using polystyrene negative resist

Polystyrene with 2000 g/mol with polydispersity Mw/Mn=1.10 was tested as negative EBL resist for contrast and resolution measurements. The powder (figure 2.2a) was purchased from Alfa Aesa and prepared as 1.2 wt/vol% solutions in chlorobenzene.

Figure 2.2 a) PS as a powder b) Spin-coater

Silicon wafer was cleaned by acetone and 2-propanol followed by O2 plasma treatment. Polystyrene film was prepared around 30 nm thickness after spin coating at 2000 rpm for 40 sec and prebaked at 60 degree for 1 hour. It has been seen that unlike high molecular weight polystyrene, low molecular weight polystyrene has formed non uniform "broken" films after baking. To resolve this problem, a thin layer of ARC (Anti Reflection Coating, from Brewer Science) has been used which is around 15 nm thickness. Crossectional view of film is shown in figure 2.3.

Figure 2.3 Crossectional view for film

2.2.1 Contrast and Sensitivity Measurement of 2K (2 kg/mol) PS

Exposure was performed by using a LEO 1530 field emission SEM equipped with Nabity Nanometer Pattern Generation System (NPGS) at acceleration voltages of 20 kV and 5 kV with 20 and 10 pA beam currents. Exposed parts of PS are insoluble in solvents since it changes its structure by crosslinking while unexposed regions are easy to be dissolved. In this study, xylene (o-, m-, p-mixed), chlorobenzene, and cyclohexane were used as developers.

After development, thickness measurement were made by AFM. Contrast was calculated by using equation $\gamma = [\log(D_{100}/D_0)]^{-1}$ where D_{100} and D_0 is defined in figure 2.4. According to Charlesby Theory, gel point which means the threshold dose where the contrast curve starts to rise (D_0) is inversely proportional to the molecular weight for the simple negative polymer resists since the number of cross-links necessary to make the resist insoluble in the developers decreases with higher molecular weight [Ku, 1969].

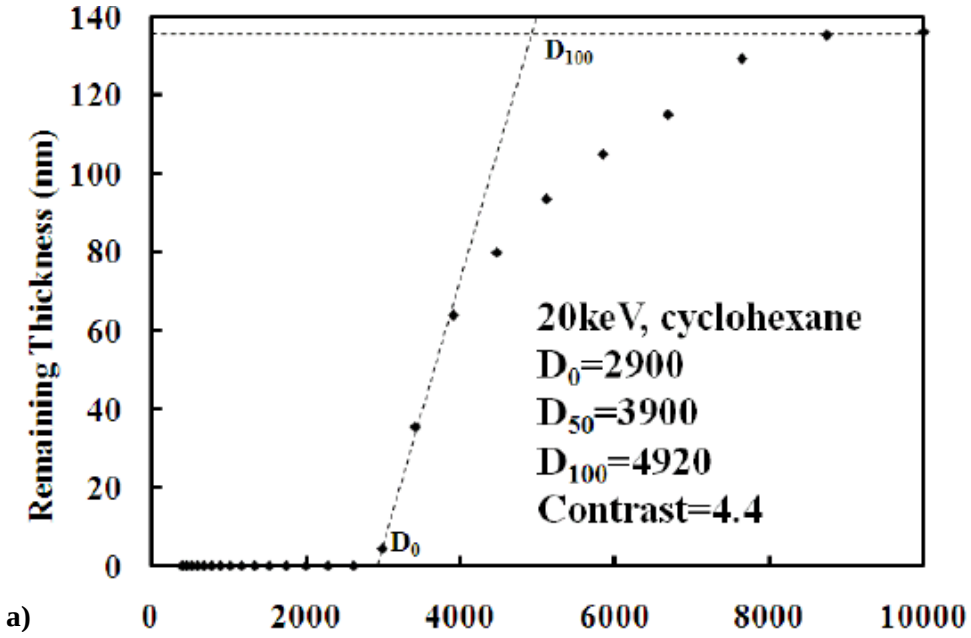

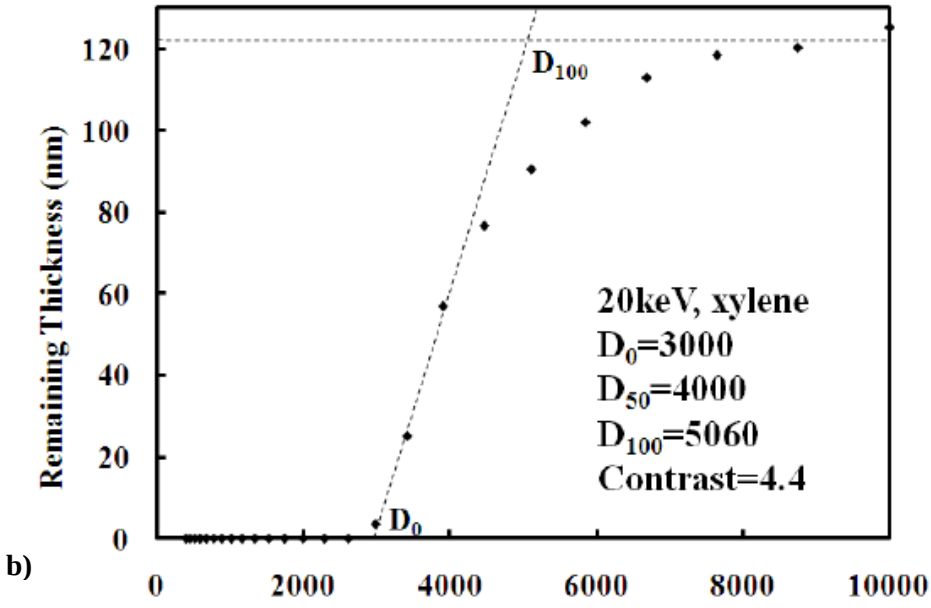

Figure 2.4 Contrast curves for PS at 20 kV exposure using a) xylene and b) cyclohexane developer

For 20 kV exposures, contrast is found to be 4.4 when developed by xylene and cyclohexane for 90 sec and rinsed by 2-propanol, and this result shows that PS has higher contrast than ZEP520 positive EBL resist**.** However, sensitivity of PS resist is rather low with D_{50}~ 4000 μC/cm^2 which is thought to limit its application to small scale nanopatterning R&D (figure 2.4). Chlorobenzene was also used as a developer but there was no apparent difference for contrast measurement. To overcome the low sensitivity, 5 kV exposure is also carried out and sensitivity was increased to D_{50}~ 1170 μC/cm^2 (figure 2.5). This is in agreement with the fact that sensitivity is roughly proportional to the e-beam energy the Bethe equation for electron energy loss in the resist E_{loss} α 1/E.log(α.E) with constant α. Sensitivity can be increased further by using higher molecular weight PS but this will reduce the resolution. Contrast was found to be 3.4 for 5 kV exposure which is close to ZEP520 resist developed at room temperature.

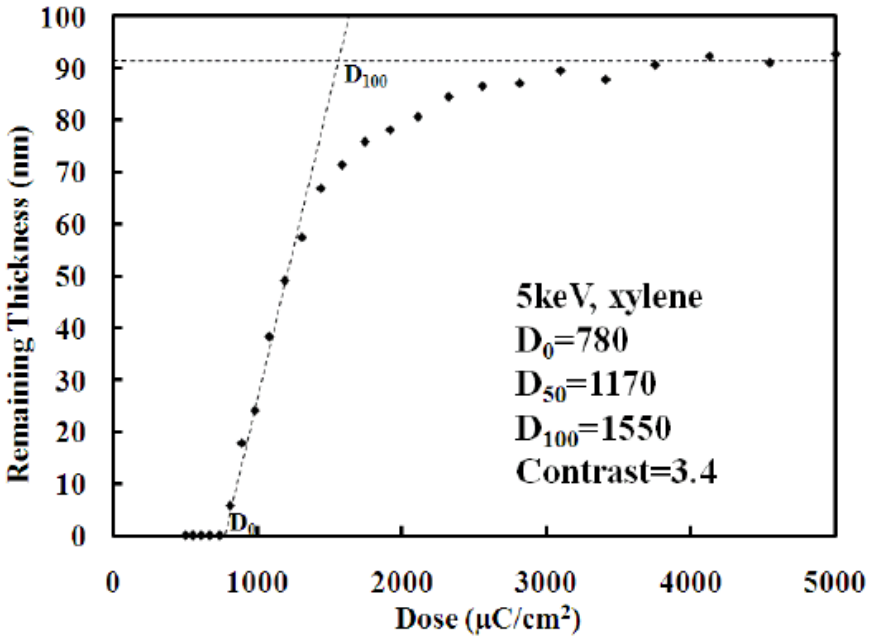

Figure 2.5 Contrast curve for 5 kV exposure and 1.5minutes xylene development for PS

2.2.2 Resolution Measurement of 2K PS

In order to study resolution of PS negative e-beam resist, we designed line arrays with different periods starting from 100 nm to 15 nm and dot array with 30 nm to 15 nm periods with NPGS. Electron beam exposure was done by using field emission SEM 1530 at 20 kV and 5 kV, 20 pA and 10 pA, and 7.7 mm and 6.5 mm working distances. For line arrays, we used different doses at range 20 nC/cm-40 nC/cm and we used xylene, chlorobenzene and cyclohexane as a developer. Developments were made at room temperature and rinsed by 2-propanol. At 5 kV exposure, uniform PS grating of 30 nm, 25 nm, and 20 nm pitch arrays were achieved with 6 nC/cm, 10 nC/cm and 4 nC/cm doses. It has been observed that type of developers used had no effect on the gratings. SEM images of line arrays developed by xylene at room temperature are shown in figure 2.6 a, b and c, and as seen the lines are very straight and smooth.

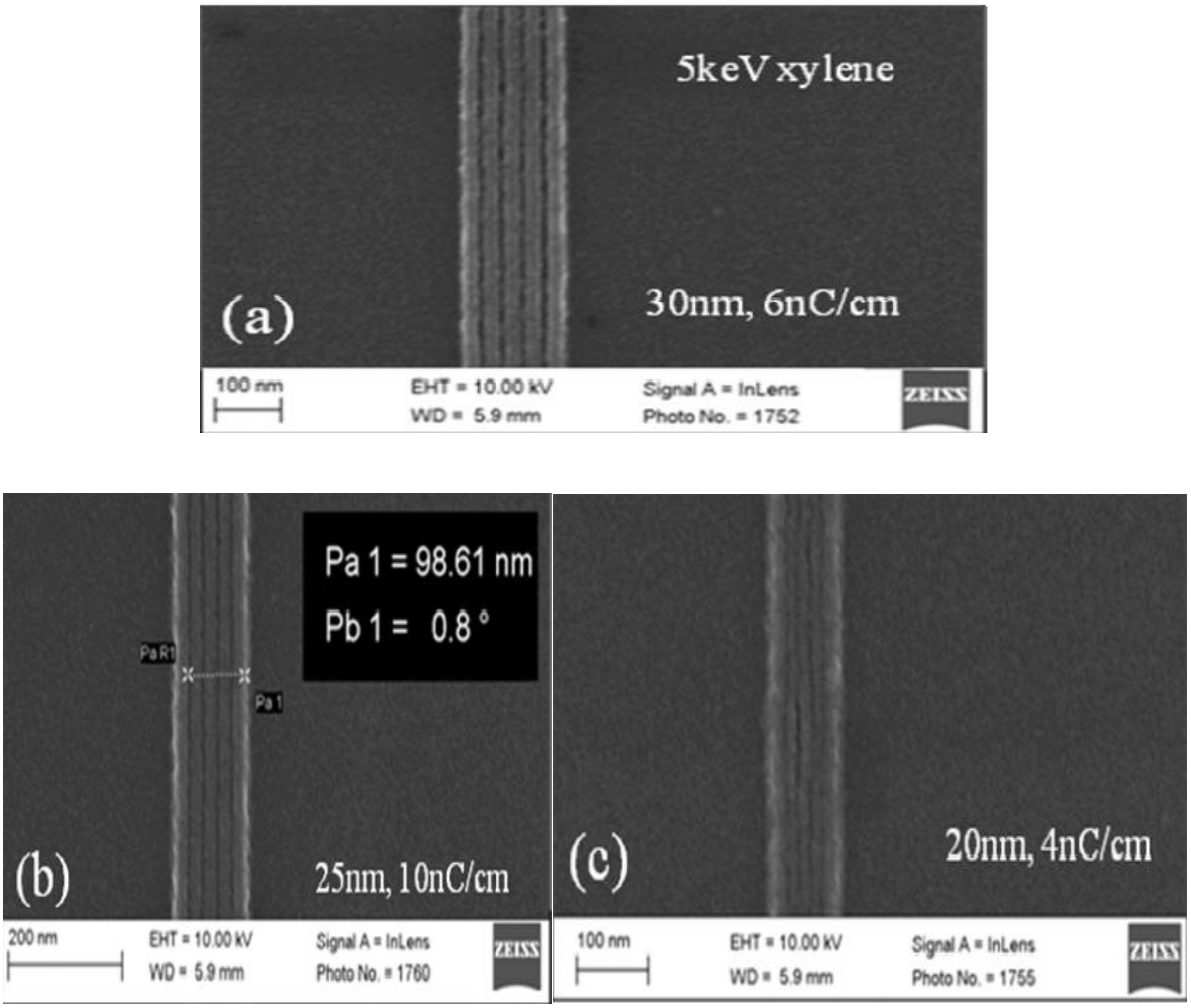

Figure 2.6 Dense line array with a period of (a) 30 nm (b) 25 nm; and (c) 20 nm. The polystyrene resist was exposed at 5 kV and developed using xylene for 1.5 min at room temperature

At 20 kV exposure, dense line arrays with a 20 nm grating were achieved. From SEM images in figure 2.7, it can be seen that there is no obvious difference occurred by different developers.

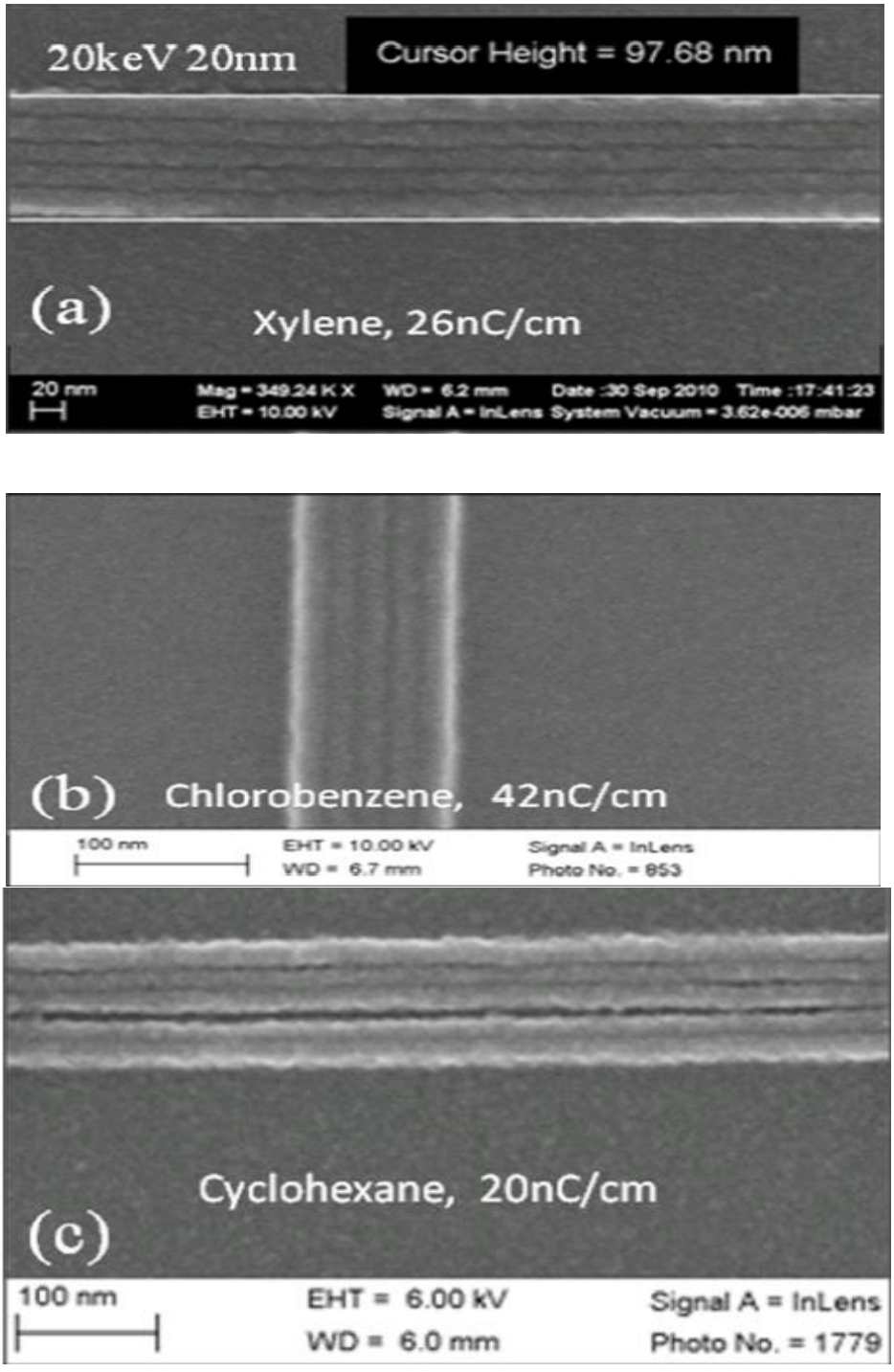

Figure 2.7 Dense line arrays with a period of 20 nm exposed at 20 kV and developed at room temperature for 1.5 min using (a) xylene; (b) chlorobenzene; and (c) cyclohexane. The lines in (c) collapsed due to capillary force during resist drying

2D dot array formation is also important for research since they can be used for data storage applications. Here (figure 2.8), dot arrays with 15 nm period were achieved by 6.5 fC/dot e-beam exposure with xylene and chlorobenzene developments followed by 2-propanol rinse.

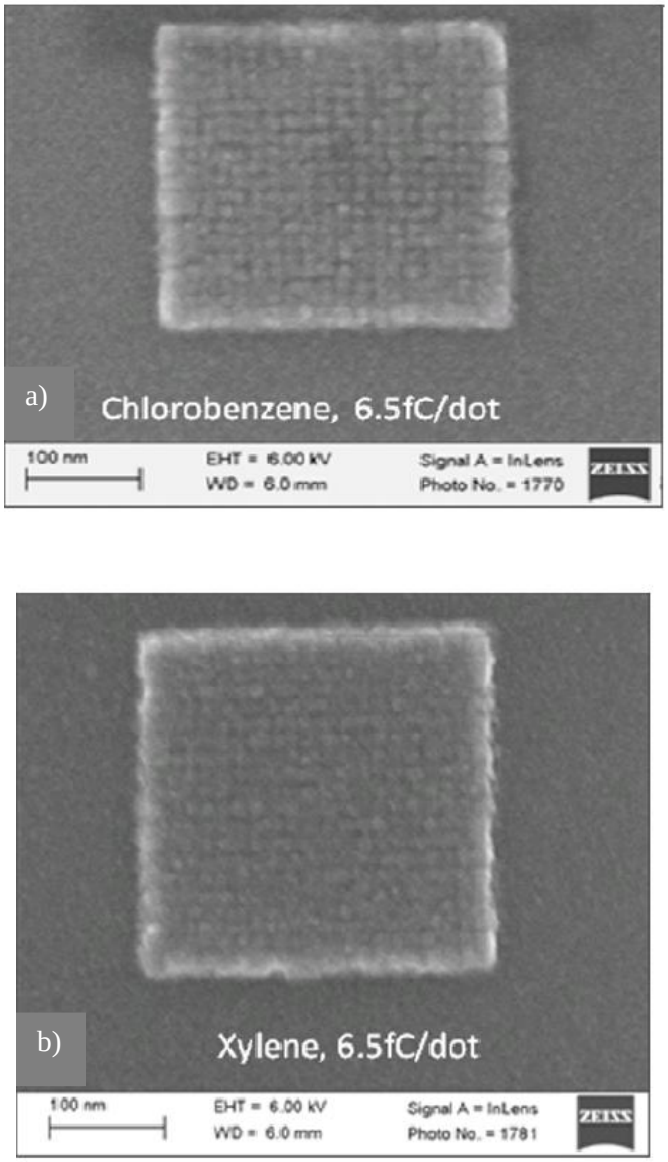

Figure 2.8 Dense 2D dot array with a period of 15 nm exposed at 5 kV and developed by a) chlorobenzene and b) xylene for 1.5 min at room temperature.

Previously, 18 nm period 2D dot arrays (corresponding to 2.0 Tbits/in^2) were achieved using ZEP resist. Our result is believed to be the highest pattern density ever obtained using organic EBL resists. However, it has poor sensitivity (4000 μC/cm^2) since more cross-links are needed to render the molecular weight Polystyrene insoluble in the developer.

After studying the high resolution EBL by using PS with molecular weight of 2 kg/mol, we have investigated possible increase in sensitivity of PS using higher molecular weight of PS as suggested by Charlesby theory. We dissolved 170 kg/mol (Mw/Mn=1.06 from Pressure Chemicals) polystyrene in chlorobenzene to obtain a film thickness of 42 nm. Exposure was carried out using a Raith 150^{TWO} tool at 5 kV acceleration voltage. After exposure, the resist was developed using tetrahydrofuran (THF) and xylene (o-, m-, p- mixed), which are both solvents for (un-cross-linked) polystyrene. Figure 2.9 is the contrast curve of polystyrene that shows sensitivity (D_{50}) of 12 μC/cm^2, which is 97x improved over the 2 kg/mol case (1170 μC/cm^2) and this is in good agreement with Charlesby theory [Ku, 1969]. The sensitivity is also an order higher than PMMA. We want to point out that this is very different from positive resist such as PMMA for which in principle the sensitivity should be independent of its molecular weight because, though longer chain needs more chain scission to render it soluble in developer, it also receives more exposure dose proportionally. The contrast of the current resist is much lower than that of 2 kg/mol polystyrene (2.0 vs. 3.4), which is expected from the fact that generally high sensitivity comes with low contrast and achievable resolution [Ocola, 2006]. To find out its high resolution capability we wrote dense line arrays with 40-200 nm period range with Raith 150^{TWO} tool at 5 kV with dose range of 0.02 to 0.45 nC/cm and developed the film by using THF for 90 seconds. SEM image of the developed resist pattern is shown in figure 2.10. As seen, we can achieve 48 nm lines with 0.45 nC/cm doses using the 170 kg/mol polystyrene resist which is a rather good resolution for high molecular weight of PS resist.

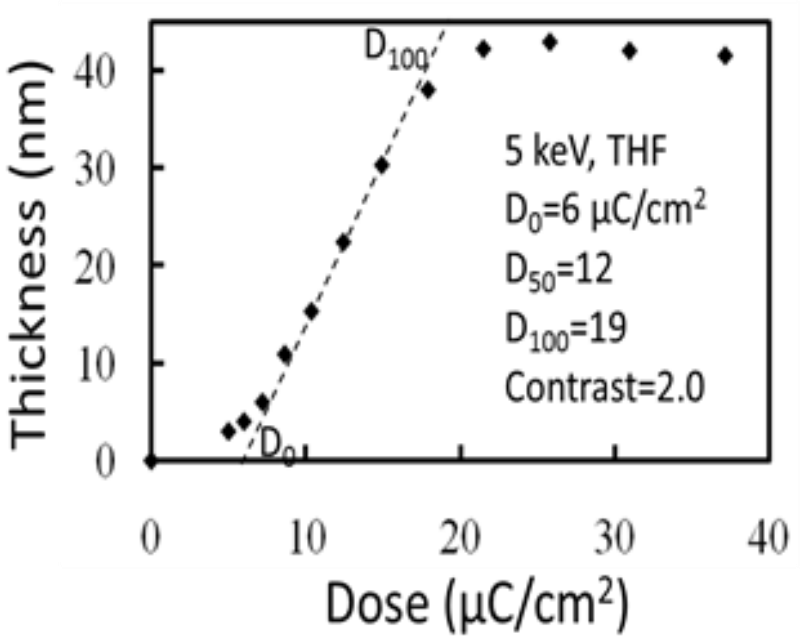

Figure 2.9 Contrast curve for 170 kg/mol polystyrene exposed at 5 kV and developed by tetrahydrofuran for 1.5 min. The contrast ($\gamma = (\log_{10}(D_{100}/D_0))^{-1}$) is calculated to be 2.0,and the sensitivity (D_{50}) is 12 μC/cm2.

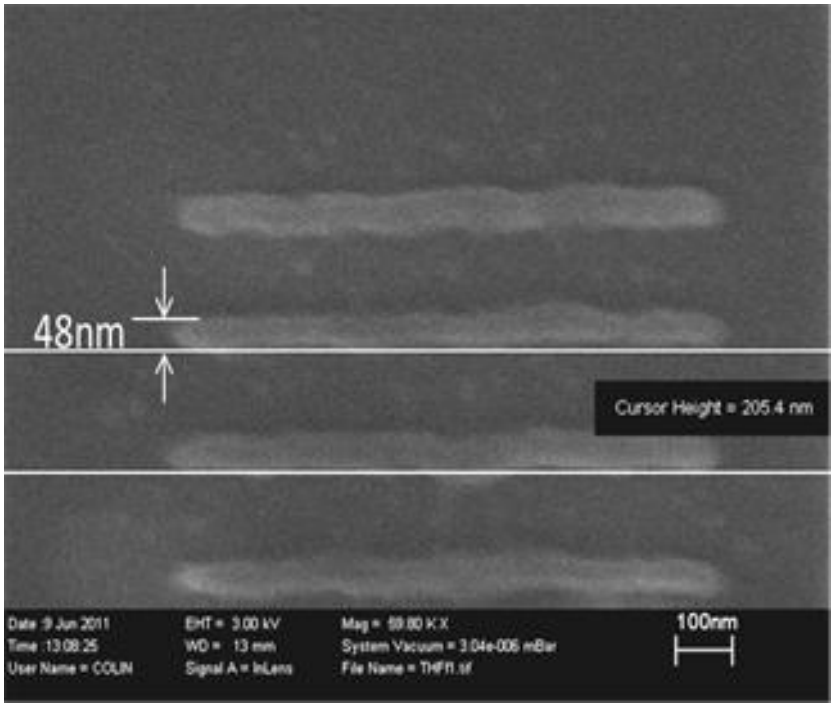

Figure 2.10 SEM image of polystyrene line array with line-width 48 nm, exposed at 5 kV and developed by tetrahydrofuran for 1.5 min.

2.3 Summary of high resolution EBL by using PS negative resist

Desirable properties for EBL resist include high sensitivity, high contrast and high dry etching selectivity to the substrate materials. Here, the exposure behaviour of low molecular weight (2000 g/mol) polystyrene as a negative tone electron beam lithography (EBL) resist was studied, with the goal of finding the ultimate achievable resolution. It demonstrated fairly well-defined patterning of a 20 nm period line array and a 15 nm period dot array, which are the densest patterns ever achieved using organic EBL resists. Such dense patterns can be achieved both at 20 kV and 5 kV beam energy using different developers. In addition to its ultra-high resolution capability of low molecular weight of PS, we also investigated resolution and sensitivity of high molecular weight (170 kg/mol) of PS as we expect that 2 kg/mol PS film has poor sensitivity and it can be increased by using high molecular

weight. We achieved great sensitivity (12 μC/cm^2) with 48 nm half pitch resolution. For future work, we will investigate resolution and sensitivity capability of PS with 900 kg/mol molecular weight.

To sum up, in addition to its ultra-high resolution capability, polystyrene is a simple and low-cost resist with easy process control and practically unlimited shelf life.

Chapter 3

Thermal Nanoimprint Lithography using Fluoropolymer Mold

3.1 Introduction

In today's technology, the ability to fabricate structures with nanoscale is extremely important, especially in semiconductor technology [Guo, 2007]. With reducing the size of the features, problems as resolution, reliability, speed, cost and overlay accuracy come out. Lithography techniques such as electron beam lithography, ion beam lithography, scanning probe based lithography and Nanoimprint lithography have been developed to overcome these issues [Chou, 1995, Grigorescu, 2009]. These lithography techniques are based on chemical reactions in certain polymers which make the polymer soluble in a solution after light or beam exposure. Among them, photolithography is popular for writing large areas which is important for integrated circuits (ICs), whereas its resolution limited by wavelength of the light being used. It is thus difficult to achieve sub-30 nm feature sizes with optical lithography. There is a demand to figure out cost of fabrication, limit of the feature sizes and practical fabrication. NanoImprint Lithography (NIL) developed by Chou in 1995 has low-cost and high throughput which makes it an alternative tool for photolithography and electron beam lithography [Chou, 1995, Chou, 1996]. After invention of NIL, there have been great efforts to achieve sub-30 nm resolution on large surfaces quickly and cost effectively in the past decades, and now NIL is capable of patterning sub-10 nm features, and it is accepted as a next generation top-down fabrication method with high throughput and low cost [Chou, 1997, Austin, 2004]. International Technology Roadmap for Semiconductors (ITRS) has announced NIL as one candidate technology for IC production [ITRS, 2003]. In this chapter, NIL will be discussed in detail.

3.2 Overview of Nanoimprint Lithography

Nanoimprint Lithography which is a mechanical way of lithography is a relatively new lithography technique with ultra-high resolution, high throughput and low cost [Khang, 2004]. First demonstration for NIL was done by Chou group in 1995 by using Poly methyl methacrylate (PMMA) resist with 10 nm feature sizes (figure 3.1), and after this achievement there has been much effort to improve the NIL capabilities [Cui, 2005]. Since there is no light diffraction or electron scattering as in photolithography and e-beam lithography, resolution of NIL depends only on the template feature size. Since there is no need for complex devices as in optical or e-beam lithography, it is a low cost technique and lithography can be done on large surfaces.

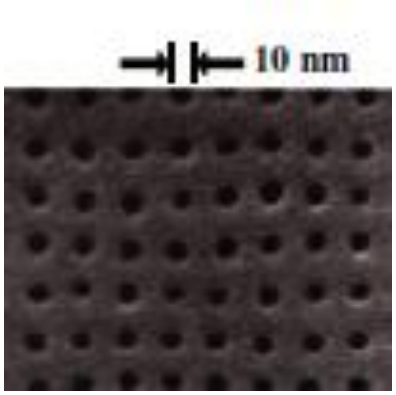

Figure 3.1 10 nm diameter and 60 nm period hole array achieved by S. Chou using NIL [Chou, 1995]

The key advantage of NIL is its capability of fabrication of structures over large area from micron to nanoscale sizes [Wang, 2010]. As a result, NIL is a promising tool in many application areas as nanoelectronics, nanooptoelectronics, data storage, electromechanical systems (MEMS/NEMS), LED (light emitting diode), quantum electronic devices, photodetectors, optical and biological devices [Wang, 2010; Zhang, 2003; Balla, 2008; Martini, 2000; Yu 1999; Lai, 2008].

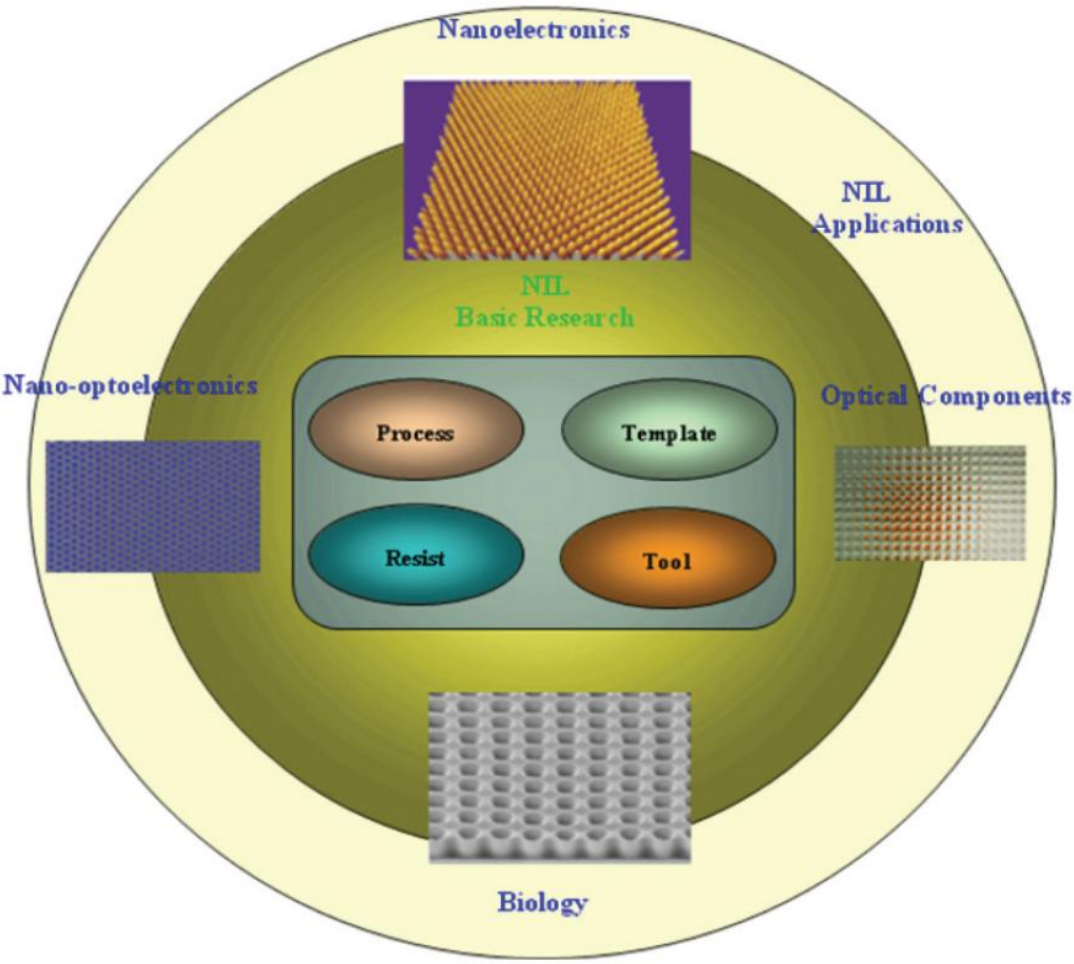

Figure 3.2 Scheme showing the application areas of NIL [Wang, 2010]

3.2.1 Principles of NIL

Principally, NIL mechanically modifies the polymer film (resist) by using a template (mold) having micro/nano sized features on it. Working principle of NIL is schemed in figure 3.3.

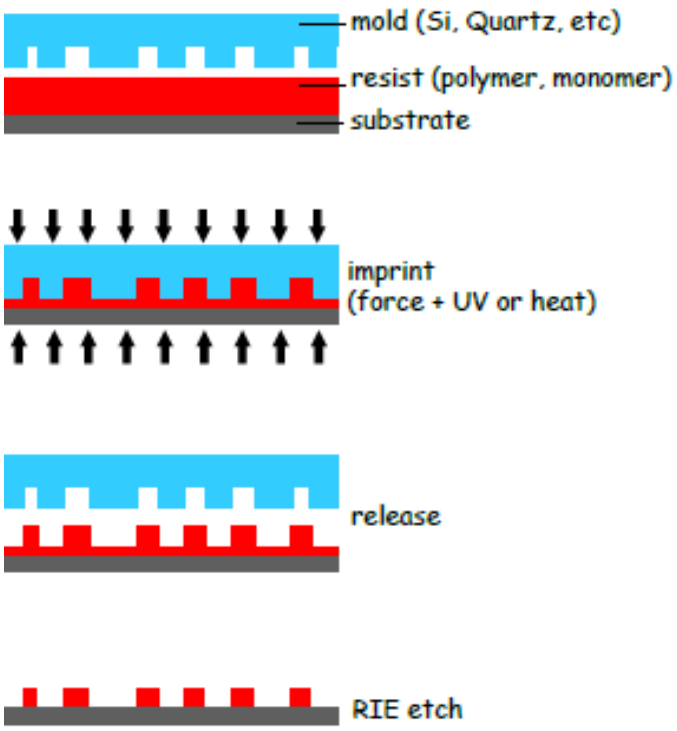

Figure 3.3 Working principle of NanoImprint Lithography: Imprint is done by whether heat treatment or UV-light exposure

Basically, there are two types of nanoimprint lithography: Thermal (T-NIL) and UV-based (UV-NIL) nanoimprint lithographies and both of them are capable of fabrication sub-10 nm features.

In Thermal NIL, a thin layer of imprint resist is spin-coated on the substrate and mold which has patterns on it is put on the substrate. Then, they are pressed together under certain pressure and heated up above glass transition temperature (Tg) of the resist. After being cooled down, the mold and substrate are separated and pattern can be transferred to substrate via RIE. Earliest thermal-NIL was done by Chou using PMMA resist and hole array mold [Chou, 1996].

In UV-based NIL, mold is usually made by transparent material like fused silica, quartz, Polydimethylsiloxane (PDMS) and substrate is covered by UV-curable liquid. After mold and substrate are pressed together, the resist is cured by applying UV light and the liquid becomes solid. After separation of the mold and substrate, similar pattern transfer can be applied as thermal-NIL process. The difference between two types of NIL is that resin that is used in UV-NIL is liquid at room temperature and shaped and cured upon pressed and UV light exposure.

3.2.2 Basics of NIL Process

The elements required for NIL are ***substrate, resists and mold***. Si, SiC, silicon nitride, metals, diamonds, SiO_2, even flexible materials are used as a substrate [Wang, 2010]. PMMA, Polystyrene (PS), Polyvinyl phenyl ketone (PVPK), SU-8, mr-I 9000E, MEH-PPV, ZEP-520, PAK01, and HSQ are just some of the popular resists for NIL process [Wang, 2010, Schift, 2008]. Since NIL makes pattern replication mechanically, the resist should be deformable under applied pressure and has good mechanical strength to keep its structural integrity during the demolding process. To be patterned well, the resist should have lower Young's modulus than the mold. Low viscosity is also important for NIL resist since during curing or heating up, the resist will start to deform which is necessary for imprinting. Anti-sticking is another concern for NIL resists because during demolding mold has to be removed from the substrate without breaking. For some applications, Reactive Ion Etching (RIE) selectivity is an important properties of the resist for NIL process.

3.2.3 NIL Mold

It can be said that the most crucial element for high resolution NIL is the mold (stamp) since the limits of resolution and pattern density is largely depend on the mold. Hence, fabrication of NIL mold is the greatest challenge for NIL process. There is a variety of features for a material to be considered as a good mold material. Mechanical strength is one of the important features of the mold, and the

material used as a mold should have high strength so that it can be pressured and demolded from the resist without being broken. On the other hand, flexibility is a major concern for some applications such as Organic Light Emitting Diodes (OLEDs), LEDs, etc. [Wang, 2010]. Thermal expansion coefficient and thermal stability are the important parameters for mechanical properties of the mold [Bhushan, 2007]. During heating, the mold and substrate will expand laterally and their expansions should be close enough to each other to maintain the imprinted pattern resolution. Other than mechanical properties, optical and chemical properties, transparency, conductivity, and anti-sticking property are important for the mold materials. Furthermore, high pattern fidelity, lifespan, and reliability of the mold are key factors since fabrication of the mold is expensive and time consuming.

Si, SiO_2, diamond, quartz, glass, and metals are usual materials for mold due to their hardness [Guo, 2007]. There are also some polymeric materials used for mold which are called as soft materials, such as Polydimethylsiloxane (PDMS), Polyvinyl chloride (PVC), Polyvinyl alcohol (PVA), Perfluoropolyether (PFPE), Ethylene tetrafluoroethylene (ETFE), and Teflon AF 2400 [Wang, 2010; Canelas, 2009; Khang, 2004]. They have relatively good mechanical strength and formability compared to other sources and some has UV transparency which is important for UV-NIL. NIL is called soft lithography once one of these materials is used as a mold.

3.2.4 NIL Tools

In this part, recent progress in NIL equipment and key components will be introduced. Currently, there are 5 different types of machines for NIL process: solid parallel plate (SPP) presses NIL, step-and-repeat NIL, Roller Type NIL, Air Cushion Press (ACP) NIL, and Electric Field Assisted NIL (EFAN) as shown in figure 3.4 [Wang 2010, Hu, 2004].

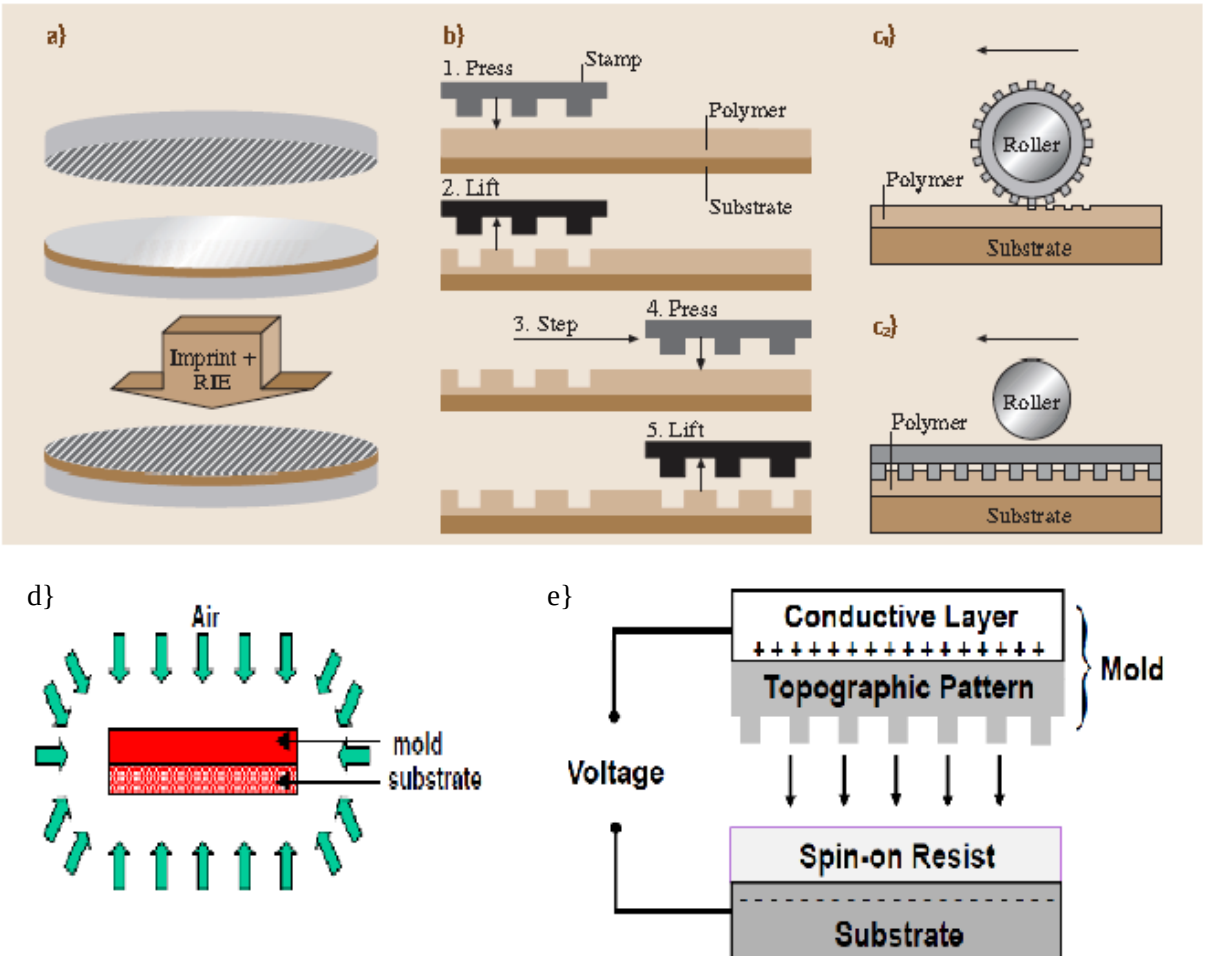

Figure 3.4 Solid Parallel Plate (SPP) system, Step-and-Repeat system, Roll-to-Roll system, Air Cushion Press (ACP) system, and Electric Field Assisted Nanoimprint (EFAN) system are five different of NIL systems [Bhushan, 2007, Hu, 2004]

Solid Parallel Plate Press system (SPPS) is a traditional NIL tool where surface of an entire wafer is patterned in one step by pressing from two sides: substrate and mold. For SPPS, mold and substrate should have same dimension. Some problems faced with SPPS are imperfect plate surfaces, non-parallelism between plates and curved sample surfaces which leads undesired pattern on the substrate or broken mold/substrate. To overcome these problems, a piece of cleanroom paper, plastics or

graphite sheet can be put above and below the mold and substrate. Air Cushion Press (ACP) system is developed by Nanonex to resolve this problem [Hu, 2004]. In ACP, shown in figure 3.4d, air pressure is applied in all directions for conformal contact and imprint, and it has ultra-uniformity with respect to SPPS.

In Step-and-Repeat NIL, small area is patterned one after the other. That is after one imprint process, stamp (mold) is moved to the next desired area to be patterned. Step-and-Repeat process has advantages that smaller area is patterned each time, and thus different molds can be used for the same substrate.

Roller Type NIL is mostly used for flexible surfaces where it has many applications in area of electronics and optical devices on flexible substrates. In Roller-type NIL systems, mold can be in a cylindrical shape so that imprint is done by moving the mold or flat shape which is rotated by the system itself.

EFAN (Electric Field Assisted Nanoimprint) system is designed to be an alternative for SPPS and ACP in order to overcome the problems as poor alignment and uniformity, and damage on mold and substrate. In EFAN, both mold and substrate have a conductive layer and electric field is generated by applied voltage which makes mold pressed onto the resist due to electrostatic force. To generate 1 atm pressure on the substrate, electric field with $5x10^5$ V/cm is needed [Liang, 2005].

There are five leading suppliers for NIL tool and process in the world: Obducat, Suss, EVG, Nanonex, and Molecular Imprints [Wang, 2010]. Obducat, Sweden based lithography tool supplier, is the first company to commercialize the NIL system [Wang, 2010, Obducat Sindre]. In figure 3.5, Sindre400® for high volume production series which has high yield and low maintenance cost is shown. Sindre® includes three embedded proprietary technologies: soft press, simultaneous UV and Thermal NIL and polymer stamp technologies. It has capability to pattern 30 wafers per hour with up

to 8 inch size wafer. Sindre® HVM (High Volume Production) is targeted for applications as LED, OLEDs, NEMS/MEMS, Displays, HDD, etc. [Obducat Sindre]

Figure 3.5 Sindre400® for high volume production series [Sindre, 2011]

Molecular Imprints, founded in Austin, Texas in 2001, has developed Imprio® 300 systems (figure 3.6), which is referred as next generation Nanoimprint lithography tool. It is known as the industry's highest resolution and lowest cost-of-ownership patterning solution for CMOS patterning and development [Wang 2010, Obducat Sindre]. It has capability of sub-32 nm half pitch resolution with sub10 nm alignment accuracy with multi-layer imprint capability.

Figure 3.6 Imprio® 300 systems [Imprio, 2011]

3.2.5 Basic Principles of Mold Fabrication

NIL molds are usually made in Si or SiO_2 substrates and patterned by other lithography tools such as photolithography, and electron beam lithography. Basic process is schematized below (figure 3.7). Firstly, resist is spun onto the substrate and lithography is done on this resist. Upon development, metal (usually Cr) is deposited as etching mask and lift off is carried out. After lift-off process, pattern is transferred to the substrate via RIE, and finally wafer is cleaned by RCA cleaning to remove all materials from the surface of the substrate.

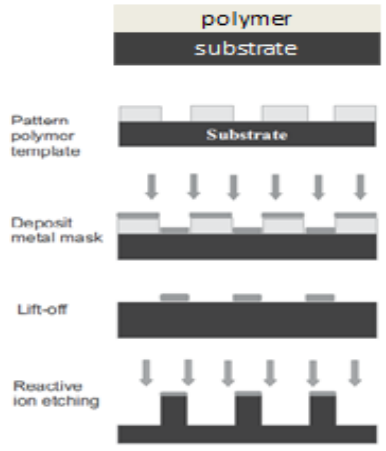

Figure 3.7 Mold fabrication steps: i) polymer film is prepared on the substrate and ii) patterned via EBL/ photolithography, iii) metal deposited on the substrate, iv) pattern is transferred via lift off, v) and RIE has been done to transfer pattern on substrate

3.3 Thermal NIL using Fluoropolymer Mold Material

3.3.1 Motivation

Nanoimprint lithography is a high throughput and high resolution molding process. Though silicon and its derivatives are still the most popular NIL mold materials, they are brittle and thus susceptible to damage. Polymer molds are more robust materials and can usually be duplicated in one molding step from a hard master mold. Therefore, it is desirable to use the polymer mold to perform the imprint, while using the expensive silicon-based mold only to duplicate the polymer mold. PDMS, PTFE, Teflon AF 2400, PMMA and PS are known materials for soft lithography. Among them, Polydimethylsiloxane (PDMS) is undoubtedly the most widely used polymer mold material since it has flexible backbone structure, high degree of toughness and large elongation. However, it is not suitable for high resolution and high aspect ratio patterning due to its low Young's modulus (1.5 MPa) [Rolland, 2004]. Its surface energy (25 mN/m) is not low enough for non-destructive

demolding, and deformations and distortions occur during fabrication due to its high thermal expansion coefficient (260 μm/m^{0}C) and thermal curing [Rolland, 2004, Truong, 2006].

Fluoropolymer, which is liquid at room temperature, can be an alternative material for soft molds [Rolland, 2004]. It is cross-linked under UV light exposure to yield elastomers with an extremely low surface energy (12 mN/m), leading to the selective filling into nanoscale cavities in the mold [Truong 2007, Canelas, 2009]. PFPE (Perfluoropolyether) is the main component of Fluoropolymer that is composed of only carbon, fluorine and oxygen (figure 3.8). PFPE is first developed in the early 1960s and used in fuel and oil resistant lubricant applications [Uniflor]. It is chemically and thermally stable therefore it swells much less than PDMS when exposed to most organic compounds. It has wide temperature range (from -40 to + 288 ^{0}C) which is important to be used as soft mold for thermal NIL. Also, Teflon like structure of the PFPE makes the organic particles to be easily removed from the mold [Canelas, 2009, Uniflor]. PFPE is a non-toxic and biologically inert. Also, it can stand for high applied pressure. Thus, PFPE has received enough attention to become a popular soft lithography mold. In this work, we investigate the potential of using a PFPE mold for thermal-NIL which is more popular than UV-curing NIL because thermal NIL has high yield and works with simple thermoplastic polymers.

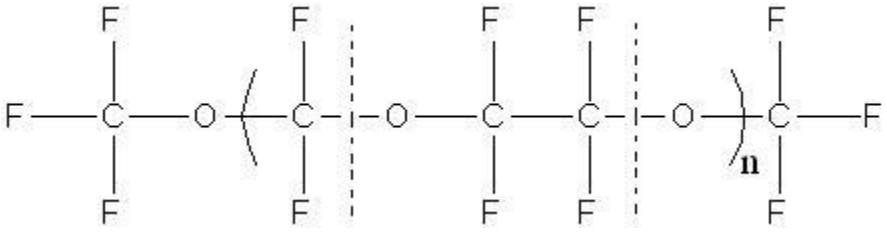

Figure 3.8 Generalized structure for PFPE (Perfluoropolyether)

3.3.2 Thermal NIL using PFPE Fluoropolymer mold

3.3.2.1 Materials Preparation

To minimize the thermal expansion mismatch that is important for thermal NIL, we used a silicon wafer (opaque to UV) as a support for the fluoropolymer layer, and accordingly replaced the photoinitiator for UV-curing with a thermal curing agent 1,1'-azobis(cyclohexanecarbonitrile) (ABCN, figure 3.9).

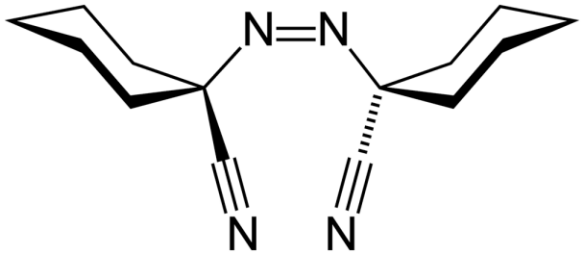

Figure 3.9 Chemical structure of 1,1'-azobis(cyclohexanecarbonitrile) (ABCN)

ABCN was dissolved in ethanol to a concentration of 0.1M, and added 1 ml of this mixture into 50 ml of Fluoropolymer MD 700 (Cornerstone Technology, Inc.). The ethanol was subsequently removed by vacuum. To test fluoropolymer as a polymer mold material for NIL, we chose a Si mold with 200 nm period and 100 nm depth grating pattern. Also, to support fluoropolymer mold we used silicon wafer. Thermal curing was carried out at 100^{o}C for 3 hours in a nitrogen environment (figure 3.10). One critical issue is the adhesion of the fluoropolymer to the silicon support, which is very poor due to the low surface energy of the fluoropolymer. It is believed that this is also an issue for UV-curing NIL, though it was not previously mentioned in the literature. This problem solved by treating the

silicon wafer with (3-acryloxypropyl) trichlorosilane (SIA0199.0 from Gelest, see figure 3.11) in vapor phase.

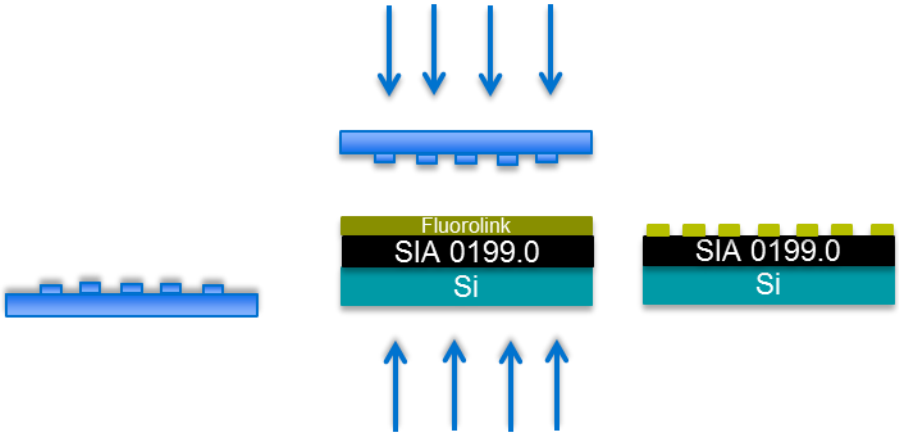

Figure 3.10 Schematic view of Fluoropolymer mold preparation

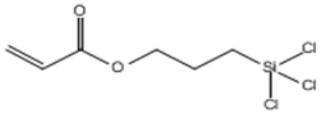

Figure 3.11 Chemical structure of (3-acryloxypropyl) trichlorosilane (SIA0199.0 from Gelest)

For thermal NIL using the fluoropolymer mold, we chose poly (vinyl phenyl ketone) (PVPK) as resist as it is 3× more resistant to plasma etching than PMMA with a relatively low glass transition temperature (58^{o}C vs. ~105^{o}C for PMMA).

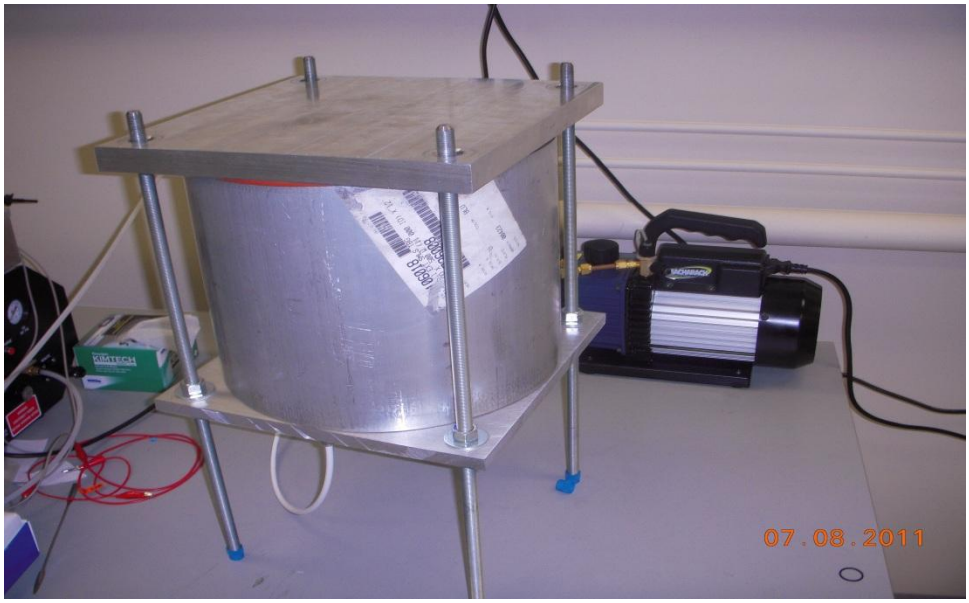

Figure 3.12 House built solid parallel plate press system (SPPS)

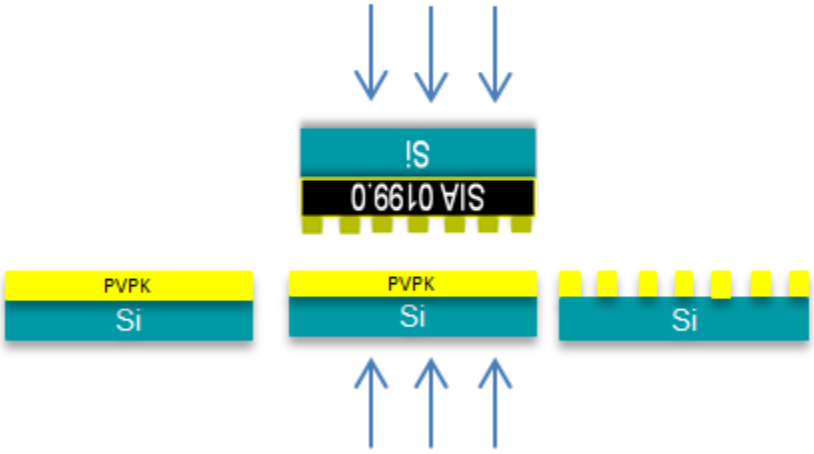

Figure 3.13 Side view of nanoimprint lithography using fluoropolymer mold

Using Solid Parallel Plate Press System made by our group (figure 3.12), the NIL process was done at 90 ^{0}C for 10 min with pressure of 7 bars. After cooling down, we released the PFPE mold from the substrate (figure 3.13). For SEM imaging, we coated 10 nm Cr on top of the substrate. Figure 3.14 and 3.15 are SEM images of a 200 nm period grating pattern over a 100 mm wafer surface. Some parts are not imprinted due to dust particles on the substrate. Once we zoomed in, we found that grating with 200 nm periods was imprinted very well (figure 3.16), though some lines are missing due to dust particles. The detail of the line-edge roughness of the master mold was duplicated into the resist, implying that the fluoropolymer mold is capable of resolution far better than 100 nm (figure 3.17).

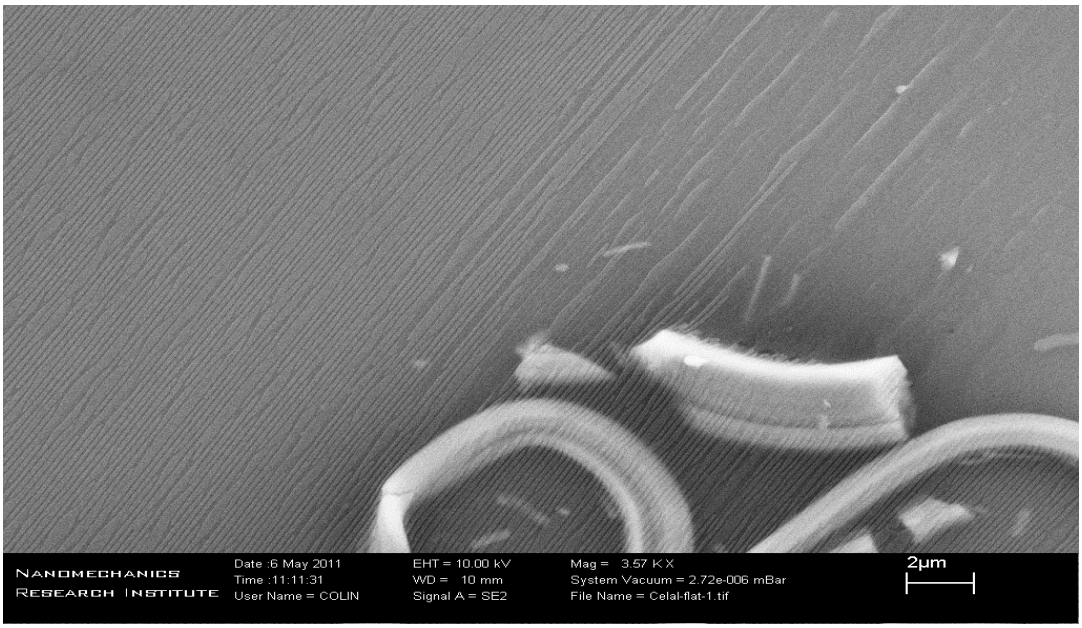

Figure 3.14 NIL result made by Fluoropolymer mold

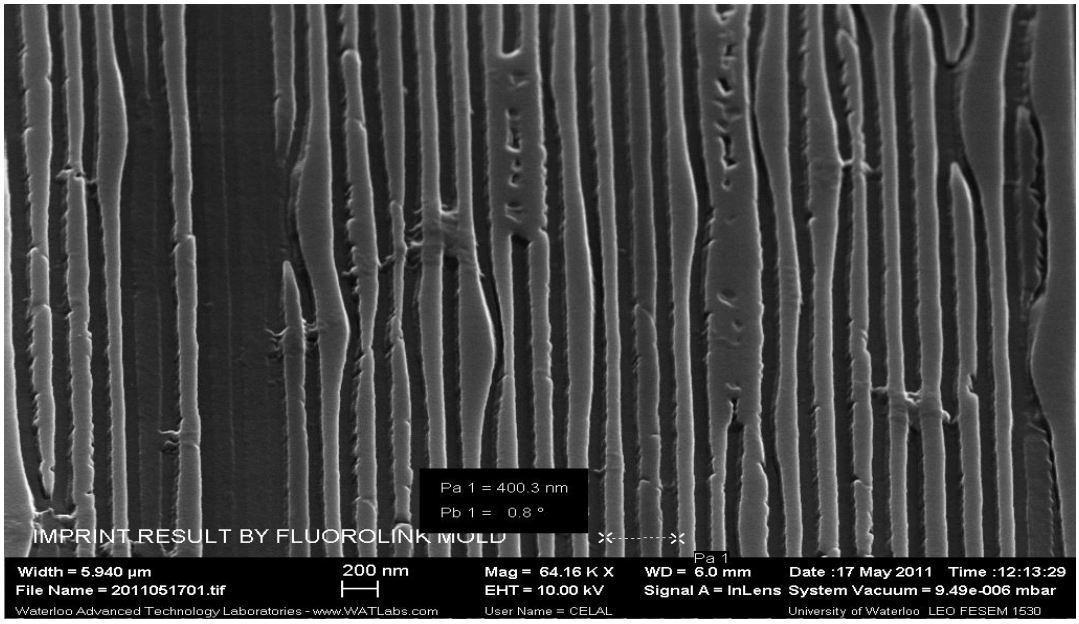

Figure 3.15 NIL result by using fluoropolymer mold on large scale. There are discrete lines due to dusty particles and inhomogeneous pressure.

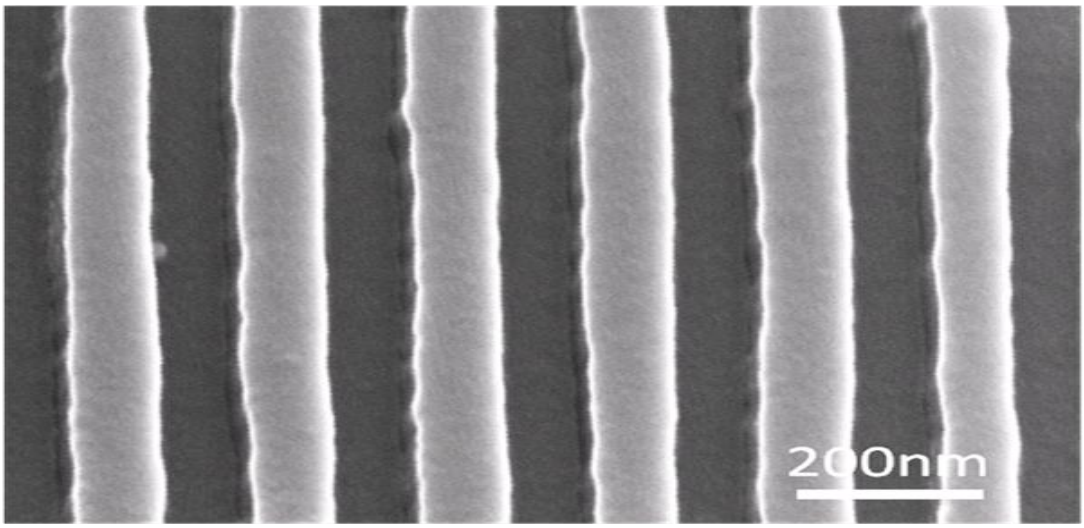

Figure 3.16 SEM image of 200 nm period grating with PVPK polymer

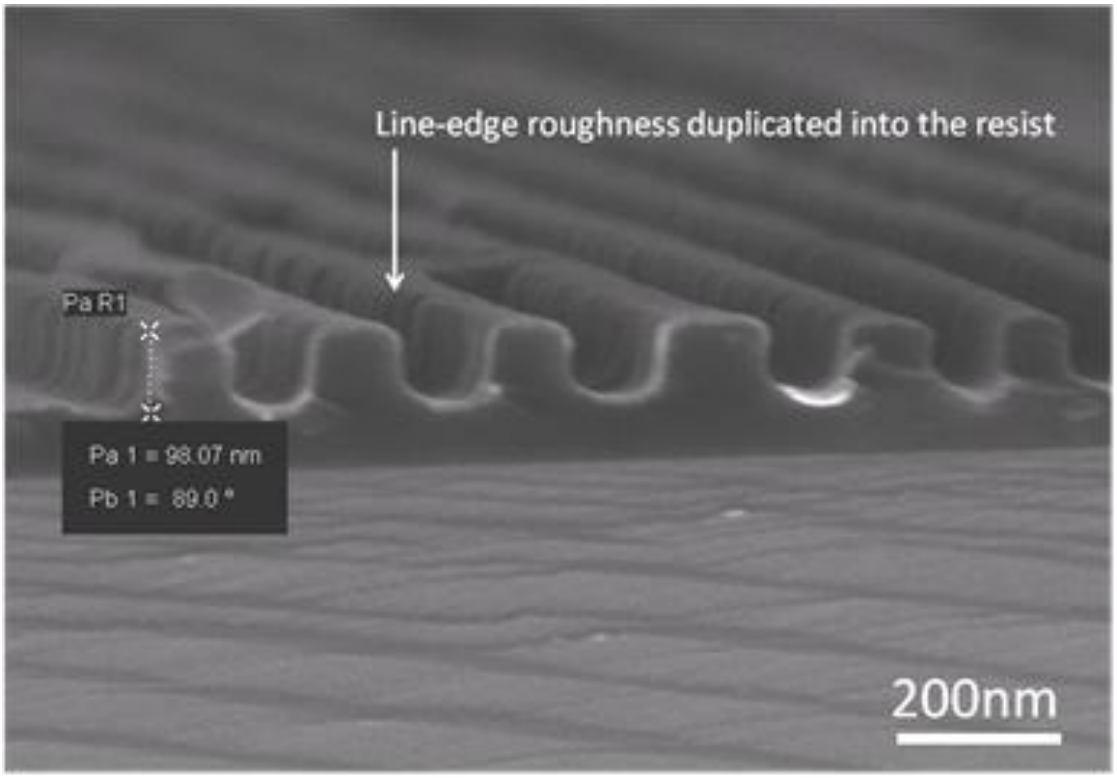

Figure 3.17 SEM image of NIL result by fluoropolymer mold. Line edge roughness is also duplicated into the resist well.

3.4 Conclusion

Nanoimprint lithography is flagged as a next generation lithography technique for nanofabrication and mold is a key component for NIL with high resolution and low cost, high fidelity and reliability. Fluoropolymer is a kind of polymeric material used as soft mold for thermal-NIL. Using fluoropolymer, we duplicated 4 inch wafer with 200 nm period with 100 nm depth of grating pattern.

Bibliography

Austin, M. D., Haixiong, G., Wei, W., Mingtao, L., Zhaoning Y., Wasserman, D., Lyon, S. A. and Stephen Y. Chou. 2004. Fabrication of 5 nm linewidth and 14 nm pitch features by nanoimprint lithography, Appl. Phys. Letter, **84**, 5299

Austin, M. D., Zhang, W., Ge, H. X., Wasserman, D. Lyon and Chou, S. A. 2005. 6 nm halfpitch lines and 0.04 μm^2 static random access memory patterns by nanoimprint lithography.Nanotechnol., **16**, 1058-1061

Balla, T. Spearing and Monk, S. A. 2008. An assessment of the process capabilities of nanoimprint lithography, J. Phys. D: Appl. Phys., **41**, 174001.

Bhushan, B. 2007. *Handbook of Nanotechnology*, Springer, Berlin Heidelberg, 2nd edition

Bilenberg, B., Jacobsen, S., Schmidt, M. S., Skjolding, L.H.D., Shi, P., Bøggild, P., Tegenfeldt, J. O. and Kristensen, A. 2001. High Resolution 100 kV Electron Beam Lithography in SU-8, Microelectronic Engineering **83** 1609–1612.

Canelas D A, Herlihy, KP and DeSimone, JM. 2009. Top-down particle fabrication: control of size and shape for diagnostic imaging and drug delivery, WIREs Nanomedicine and Nanobiotechnology, Advanced Review, Vol.**1**.

Chang T. H. P. 1975. Proximity Effect in electron beam lithography. J. Vac. Sci. Technol. **B 12 (6)**, 1271

Chou S. Y., Krauss, P.R., Zhang, W., Guo, L. J. and Zhuang, L. 1997. Sub-10 nm imprint lithography and applications, J. Vac. Sci. Technol. B **15**, 2897

Chou S. Y., Krauss, P. R. and Renstrom P. J. 1996. Nanoimprint lithography. *J. Vac. Sci. Technol.* **B 14**, 4129

Chou S. Y., Krauss, P. R. and P. J. Renstrom. 1996. Imprint lithography with 25-nanometer resolution. *Science* **272**, 85

Chou S. Y., Krauss, P. R. and Renstrom, P. J. 1995. Imprint of sub-25 nm vias and trenches in polymers. Appl. Phys. Letter, **67**, 3114

Cord, B. 2009. *Achieving Sub-10-nm Resolution using Scanning Electron Beam Lithography*. PhD Thesis, Massachusetts Institute of Technology, Massachusetts, Boston, US

Cui Z. 2005. *Micro-Nanofabrication*, Springer

Feynman, R. P. 1960. There is plenty of Room at the Bottom, an invitation to enter a new field of physiscs Eng. Sci. Mag. **23** 143

Fujita, J., Ohnishi, Y., Ochinai, Y., Nomura, E. and Matsui, S. 1996. Nanometer-scale resolution of calixarene negative resist in electron beam lithography. J. Vac. Sci. Technol. **B 14** 4272

Gemma R. S. 2008. *Electron Beam Lithography for nanofabrication*, Phd Thesis,Universitat Autonoma de Barcelona, Barcelona, Spain

Grigorescu, A. E. and Hagen, C. W. 2009. Resists for sub-20-nm electron beam lithography with a focus on HSQ: state of the art. Nanotechnol., **20**, 292001

Guo L J. 2007. Nanoimprint Lithography: Methods and Material Requirements, Advanced Materials, **19**, 495-513

Gwyn C. W., Stulen, R., Sweeney, and D. Attwood, D. 1998. Extreme ultraviolet lithography, J.Vac. Sci. Technol. B, Vol. **16**, pp. 3142-3149

Hua Tan, Linshu K., Mingtao L., Colby S. and Larry K. 2004. Current Status of Nanonex Nanoimprint Solutions, SPIE

ITRS (International Technology Roadmap for Semiconductors). 2003. URL: http://public.itrs.net

Khang D. Y., Lee, H. H. 2004. Sub-100 nm patterning with an amorphous fluoropolymer mold Langmuir, **20**, 2445

Khang D. Y. and Khang, D. 2004. Low-Pressure Nanoimprint Lithography, Nanoletters, Vol.**4**, No.4, 633-637

Ku, H. Y. and Scala, L. C. 1969. Polymeric electron beam resists. J. Electrochem. Soc.,**116**, 980-985.

Lai K L., Leu I. C. and Hon M. H. 2009. Soft imprint lithography using swelling/deswelling characteristics of a polymer mold and a resist induced by a poor solvent, J. Micromech. Microeng. **19**, 037001

Liang X, Wei Zhang, Mingtao Li, Qiangfei Xia, Wei Wu, Haixiong Ge, Xinyu Huang, and Stephen Y. Chou. 2005. Electrostatic Force-Assisted Nanoimprint Lithography (EFAN), Nanoletters, 2005, Vol. **5**, No. 3, 527-530

Ma S., Con C., Yavuz M. and Cui B. 2011. Polystyrene negative resist for high-resolution electron beam lithography. Nanoscale Research Letters. **6**:446

Madou, Mark, J. 1997. *Fundamentals of Microfabrication.*, CRS Press

Martini I, Eisert D, Kamp, M., Worschech, L., Forchel, A. and Koeth, J. 2000. Quantum Point Contacts fabricated by nanoimprint lithography. Appl. Phys. Lett., **77**, p.2237

Moore, G.E. 1965. Cramming more components onto integrated circuits, Electronics **38** (8)

Newman, T. 1986. Tiny tale gets grand, California Institute of Technol. J. Eng. Sci. **49** 24

Nishida, T., Notomi, M., Iga R and Tamamura, T. 1992.Quantum wire fabrication by e-beam lithography using high-resolution and high-sensitivity e-beam resist ZEP-520. Jpn.J.Appl.Phys., **31**,pt.1,No.12B,p.4508

Obducat Sindre. 2011. URL: http://www.obducat.com/Sindre%C2%AE-489.aspx

Ocola L. E. and A. Stein. 2006. Effect of cold development on improvement in electron-beam nanopatterning resolution and line roughness. *J. Vac. Sci. Technol. B*, **24**(6), 3061

Pain L., Icard, B., Manakli, S., Todeschini, J., Minghetti, B., Wang, V and Henry, D. 2006.Transitioning of direct e-beam write technology from research and development into production flow, Microelectronic Engineering, Vol. **83** , pp. 749–753

Rolland J. P., Hagberg, E C, Denison, G M, Cater K R. and Desimone J M. 2004. Functional perfluoropolyethers as novel materials for microfluidics and soft lithography. Angew. Chem. Int. Ed. **43**, 5796-5799

Saavedra H M, Mullen T J, Zhang P, Dewey D C, Claridge S A and Weiss P S. 2010. Hybrid strategies in nanolithography. Rep. Prog. Phys. **73** 036501

Schift H. 2008. Nanoimprint Lithography: An old story in modern times? A review, J. Vac. Sci. Technol. B **26** (2)

Semprez O. 2000. *Excimer Lasers for future lithography light sources*, Page 255, Solid State Technology.

Truong T T, Lin, RS., Jeon, S., Lee H.H., Maria, J., Gaur, A., Hua, F., Meinel, I. and Rogers, J.A. 2007. Soft Lithography Using Acryloxy Perfuloropolyether Composite Stamps, Langmuir, **23**, 2898-2905

Tseng, A. A.2004. Recent developments in micromilling using focused ion beam technology. J. Micromech. Microeng. **14**(4), R15-R35

Uniflor 2011.URL: http://www.nyelubricants.com/_pdf/UniFlor/uniflor_brochure_english72.pdf

Wang M. 2010. *Lithography*, Intech

Wiederrecht G. 2010. *Handbook of nanofabrication*, Elsevier

Yamamoto J., Murai F., Someda, Y., and S. Uchino. 2000. Fine Pattern Fabrication below 100 nm with 70 kV Cell Projection Electron Beam Lithography, Jpn. J. Appl. Phys., Vol.**39**, pp. 6854-6860

Yang W K J, Cord B, Duan HG, Berggren K.K., Nam, S.W., Klingfus, J., Kim K. B. and Rooks, M. J. 2009.Understanding of hydrogen silsesquioxane electron resist for sub-5-nm-half-pitch lithography, journal of vacuum science& technology B, vol **27** issue 6

Yu, Z, Schablitsky, S J and Chou, S. Y. 1999. Nanoscale GaAs metal-semiconductormetal photodetectors fabricated by nanoimprinting lithography. Appl. Phys. Lett., **64**, p.2381.

Zhang W., S. Y. Chou. 2003. Fabrication of 60-nm transistors on 4-in. wafer using nanoimprint at all lithography levels. Appl.Phys. Lett., **71**, 1881

Zhou W. 2007. *Scanning microscopy for nanotechnology: techniques and applications*, Springer.